

Rapid subglacial streamlined bedform formation at a calving bay margin

Journal:	<i>Journal of Quaternary Science</i>
Manuscript ID	JQS-15-0169.R2
Wiley - Manuscript type:	Research Article
Date Submitted by the Author:	n/a
Complete List of Authors:	Dowling, Thomas; Lund Univeristy, Department of Geology Möller, Per; Department of Geology, Quaternary Sciences, Lund University Spagnolo, Matteo; University of Aberdeen , Geography & Environment Department
Keywords:	streamlined terrain, drumlin, calving bay, De Geer moraine, ice recessional history

SCHOLARONE™
Manuscripts

1
2
3 **1 Rapid subglacial streamlined bedform formation at a calving bay**
4 **margin**
5
6

7 THOMAS P.F. DOWLING^a, PER MÖLLER^a and MATTEO SPAGNOLO^b
8
9

10
11 ^aDepartment of Geology, Quaternary Sciences, Lund University, Sölvegatan 12, SE 22362
12 Lund, Sweden. ^bGeography & Environment Department, School of Geosciences, University
13 of Aberdeen, Aberdeen AB24 3UF, UK
14
15
16
17

18
19 **ABSTRACT:** Using the LiDAR derived Swedish national height model we have identified
20
21 previously undescribed shallow streamlined glacial bedforms, small-scale drumlins, on the
22
23 Närke plain in south-central Sweden. These drumlins could only be detected with high
24
25 resolution LiDAR, due to both their subtle size and forest cover. In this area the ice margin
26
27 receded in a subaqueous environment with a proglacial water depth in the order of 100 m
28
29 during the last deglaciation. As indicated by the configuration of marginally formed De Geer
30
31 moraine ridges draping the drumlinoids, the receding ice margin formed deeply indented
32
33 calving bays. These were located around subaqueous outlets of the subglacial melt-water
34
35 drainage, with their apex position marked geomorphologically by beaded esker ridges. The
36
37 mapped small-scale drumlins are aligned perpendicular to the reconstructed ice sheet margin
38
39 and suggest formation along flow lines adjusted to the configuration of these calving
40
41 embayments as they propagated up-flow with ice margin retreat. Based on these geometric
42
43 relationships we argue that the emplacement of the drumlins was near-marginal, ~7.7-1 km
44
45 from the margin, on a short timescale (~5-35 years).
46
47
48

49
50
51 **Running title:** Flow reorganisation at calving bay margin quickly constructs drumlins.
52
53

54 **KEYWORDS:** streamlined terrain, drumlin, calving bay, De Geer moraine, ice recessional
55 history

56 Correspondence to T. P. F. Dowling, as above

57 E-mail: tom.dowling@geol.lu.se
58
59
60

27 Introduction

28 Streamlined subglacial bedforms, such as drumlins, are common geomorphic features on the
29 relict ice beds of formerly glaciated regions. As such, they have drawn intense research
30 attention as their formation is considered key for understanding ice sheet dynamics. Many
31 theories, widely inspired by various morphometric and sedimentological observations, have
32 been put forward regarding the formation of drumlins, but the debate is far from closed (see
33 discussions in, e.g., Clark, 2010; Stokes et al., 2011; Eyles et al., 2016; Möller and Dowling,
34 2016). Two aspects of key relevance that have perhaps seen relatively less attention,
35 especially in recent years, are *where* drumlins form with respect to the ice margin and the *time*
36 *frame* in which they form.

37 From a process point of view the location of formation for a drumlin must meet some
38 combination of sediment erosion, transport and/or deposition. These three elements are in turn
39 dependent on a number of things, including basal ice flow velocity and the induced basal
40 shear stress on the subglacial sediment. The latter is highly dependent on the effective stress
41 (normal stress reduced by pore water pressure) induced by the glacier at its bed. All of these
42 parameters will vary along any given flow line and the resulting criteria for drumlin formation
43 may be met sporadically or continuously throughout time. There are thus likely to be zones
44 where basic conditions for bedform formation are met better than in other places due to
45 presence of obstacles and/or a significant sediment supply (Stokes et al., 2013).

46 Drumlins are often described as forming within the main body of ice sheets (Raukas and
47 Tavast, 1994), generally in areas of fast flow (ice streams) and at significant distances from
48 the margin (Wellner et al., 2001). However, other studies suggest that they may also form
49 relatively close to ice margins (Menziés, 1979). For example, Glückert (1973, 1987) describes
50 drumlin fields in the central lake district of Finland that form outwards diverging flowsets
51 along flow lines adjusted to the lobate configuration of the Younger Dryas ice-marginal zone,
52 less than 100 km from that ice margin and over a single short ice streaming event. Other
53 examples of near-marginal streamlining include the SE Baltic where Lamsters and Zelčs
54 (2014) show that drumlins form flow sets that diverge towards strongly lobate ice-marginal
55 positions, as marked by end moraine zones. More recently at Múlajökull, Iceland, Johnson et
56 al. (2010) have suggested that drumlins might form at the very margin of a surging glacier.

57 There is relatively little in the literature that considers the chronological aspect of drumlin
58 formation as there is both a dearth of syn-formational observations and a lack of dateable

1
2
3 59 material within the features themselves. However, the time period in which a feature forms is
4 60 a critical component in efforts to reconstruct past ice sheets from the relict landscape. Of the
5 61 evidence thus far gathered there is a wide disparity in suggestions of how fast or over which
6 62 time frames subglacial bedforms are formed; Hättestrand et al. (2004) have suggested that
7 63 large drumlins in northern and central Sweden are the result of sediment accretion from
8 64 multiple glaciations and therefore have a very long formation time. In contrast to this, Smith
9 65 et al. (2007) and King et al. (2009) found that the formation of contemporary subglacial
10 66 features under an Antarctic ice stream are formed and evolve on the time scale of a few years.
11 67 Rapid formation times are also suggested from the work of Johnson et al. (2010).

12
13
14
15
16
17
18
19 68 In this paper we investigate the time of formation of a number of small drumlins mapped
20 69 within the streamlined terrain on the Närke plain, an area situated in south-central Sweden
21 70 (Fig. 1), using high-resolution LiDAR-derived topographic data. The spatial association of
22 71 these smaller features with nearby esker and De Geer moraine complexes is here investigated.
23 72 In particular, the geometry of these landforms, their relationships with both one another and
24 73 to the Swedish varve chronology, all provide an indication of where the small-scale drumlins
25 74 formed in relations to the retreating margin of the Fennoscandian Ice Sheet and the amount of
26 75 time it took them to form.

27 28 29 30 31 32 33 76 **Regional and local geologic setting of the study area**

34
35
36 77 The Närke plain in the Kumla–Örebro area, south-central Sweden (Fig. 1), on which the
37 78 drumlins investigated here are located, is a low-elevation area at ~30-80 m above present-day
38 79 sea level (m a.s.l.). Below the covering Quaternary deposits are down-faulted and tilted blocks
39 80 of crystalline basement, overlain in varying occurrence by Palaeozoic sandstone, clay slate,
40 81 alum shale and limestone, in that stratigraphic order (Ericsson, 1979).

41
42
43
44
45 82 During the deglaciation of the Kumla–Örebro area (Fig. 1), the subsequent northwards ice
46 83 recession was primarily subaqueous with the retreating ice margin standing in water depths
47 84 often in excess of 100 m (sea level at deglaciation, c. 150-160 m a.s.l. (Fig. 1), minus present-
48 85 day elevation). The area was deglaciated in conjunction with a marine ingression from the
49 86 west into the Baltic Basin (Brunnberg, 1995) a few hundred years after the final drainage of
50 87 the Baltic Ice Lake at Mount Billingen (11.62 cal ka BP according to Stroeven et al. (2015).
51 88 Thus, at deglaciation the water basin in front of the receding ice margin changed from
52 89 freshwater conditions to marine with the onset of the Yoldia Sea (Brunnberg, 1995; J. Björck

1
2
3 90 et al., 2001). This saline environment is indicated by the occurrence of the marine mollusc *Portlandia*
4 91 (*Yoldia*) *arctica* in the lowermost clay of the area (Bergdahl, 1961). Also due to the marine
5
6 92 environment at deglaciation, suspended clay was prone to flocculation (Krank, 1973; Skei and
7
8 93 Syvitski, 2013) resulting in poorly developed (symmict) varves or close to massive clay, thus
9
10 94 making a complete annual varve reconstruction, based on clastic rather than symmict varves,
11
12 95 not possible for this area. Indeed, Nilsson (1968) reports a maximum of only 48 annual
13
14 96 varves from the area within the basal section of the up to 5-10 m thick fine-grained
15
16 97 subaqueous deposits, which was not enough to construct a detailed varve chronology.

17
18 98 Varved clay chronology is based on the between-site lateral correlation of peaks in vertically
19
20 99 measured and graphically plotted summer/winter bed thicknesses for specific sites; the
21
22 100 ‘classical’ method as described in De Geer (1940) is to count the difference in basal ‘missing’
23
24 101 varves between two sites which then is a measure of difference in deglaciation age in years
25
26 102 between the two sites. From these differences in deglacial age, varve isochrones are
27
28 103 interpolated; in the case of the varve chronology from the Stockholm-Uppsala area (Fig. 2)
29
30 104 this was done in 20 year steps. The basal varves formed close to the receding ice margin and
31
32 105 the constructed varve isochrones thus mirror not only deglaciation time but also the
33
34 106 configuration of the ice margin in temporal steps during continuous ice margin recession.

35
36 107 In addition to the Stockholm-Uppsala chronology northeast of our study site a detailed and
37
38 108 precise varved clay chronology has been reconstructed just south of our investigated area,
39
40 109 between Västergötland (Strömberg, 1994) and Närke/Östergötland (Brunnberg, 1995; J.
41
42 110 Björck et al., 2001). This chronology can be extended to provide an overall indication of the
43
44 111 deglaciation time just south of the Kumla–Örebro region. The -1200 varve isochrone of
45
46 112 Brunnberg (1995) trends directly south of Kumla (Fig. 1) and the deglaciation of the Kumla–
47
48 113 Örebro area should thus have occurred between the -1200 and -1100 isochrones. As the ‘zero
49
50 114 year’ (± 0) in the Swedish time scale is set to 10 090 cal yr BP (Stroeven et al., 2015), this is
51
52 115 equivalent to c. 11.3 – 11.2 cal ka BP (Stroeven et al., 2015) as an approximate deglaciation
53
54 116 age for the Kumla–Örebro area.

55
56 117 Eskers in the area have a general S-N trend on the Närke plain (Fromm, 1972; Ericsson,
57
58 118 1979). This concurs with the general glacial striae pattern, varying between N10°W and N10
59
60 119 °E, and the primary drumlin flow sets, indicating the regional ice flow direction (Möller and
120 Dowling, 2016). The eskers occur with 4 to 9 km wide gaps between them, as calculated from

1
2
3 121 7 eskers identified from the Quaternary deposits maps of the area (Fromm, 1972; Ericsson,
4 122 1979) over a 40 km long profile from west to east. Central through the Kumla–Örebro area
5 123 runs the Hallsberg–Kumla esker; although this is the ‘official’ name (Bergdahl, 1961), it will
6 124 in the following be called the ‘Kumla esker’ for short. Parts of these eskers formed infra-
7 125 marginally as subglacial tunnel fillings, but most of the glaciofluvial sediment was deposited
8 126 as tunnel mouth subaqueous fans of varying widths lined up after each other as the ice margin
9 127 retreated (De Geer, 1897). Such types of eskers, along with more modern facies models for
10 128 their formation, have been described as beaded eskers by Bannerjee and McDonald (1975) or
11 129 as subaqueous short bead fan eskers by Warren and Ashley (1994).

12
13
14
15
16
17
18
19 130 A frequently occurring feature at deglaciation in this part of Sweden was the formation of
20 131 large, often highly indented calving bays that during their existence were closely associated
21 132 with the larger eskers of south-central Sweden. The first description of these paleo-bays was
22 133 as early as Frödin (1916), who named them ‘glaciofluvial estuaries’ due to their connection to
23 134 eskers. The more general concept of calving bays at subaqueously retreating ice margins was
24 135 introduced by Hoppe (1948, 1957) for the Fennoscandian Ice Sheet. Calving bays formed
25 136 close to the larger eskers due to intensified – possibly intermittent – calving (see later
26 137 discussion), induced at, and lateral to, the mouth of subglacial drainage channels which also
27 138 were depocenters for the formation of De Geer eskers. The calving bays propagated
28 139 backwards, following the general retreat of the ice margin. The outlines of such calving bays
29 140 are often indicated from striae on bedrock outcrops close to the larger eskers and the
30 141 orientation of near-by De Geer moraines (Strömberg, 1981). The older regional-flow striae
31 142 from north to south are often then seen to be cut by younger striae coming from ~NE, east of
32 143 the eskers, and from ~NW, west of the eskers (e.g., as described in fig. 3 in Magnusson
33 144 (1984)). Examples of calving bays associated with eskers from the Stockholm-Uppsala
34 145 region, not far from the studied Kumla–Örebro area, are shown in Fig. 2 (reproduced from
35 146 Strömberg, 1989). Here, calving bays of varying depths into the receding ice margin are also
36 147 indicated from the configuration of reconstructed ice recession lines, in turn based on data
37 148 from varve measurements (varve isochrones) (e.g. Strömberg, 1981, 1989).

38
39
40
41
42
43
44
45
46
47
48
49
50
51 149 The strongest indicator for the existence of calving bays around eskers is, however, the
52 150 configuration of subaqueously formed ice-marginal moraines, generally known as De Geer
53 151 moraines (e.g. Lindén and Möller, 2005). These moraines occur in a bimodal distribution in
54 152 Sweden, one population is located in the coastal area of north-eastern Sweden and the other as
55 153 a broad belt across the deglacial subaqueous part of south-central Sweden (Fredén, 2009; map

1
2
3 154 on p. 134; Bouvier et al., 2015). A significant pattern for this southern De Geer moraine belt
4 155 is that that the ridges at a distance from the eskers are arranged approximately perpendicular
5 156 to the esker trends, regional striae direction and drumlins, while closer to the esker ridges they
6 157 usually turn in orientation, coming in at an increasingly oblique angle to an esker on both
7 158 sides. This relationship is seen from the Quaternary deposits map of the Kumla–Örebro area
8 159 (Fromm, 1972) (Fig. 3A) and is highlighted by the extraction of De Geer moraines and striae
9 160 (Fig. 3B). This pattern has also been described from studies of aerial photographs over the
10 161 area in the past (Bergdahl, 1959, 1961, 1965). Taken together, the geometric relationship
11 162 between De Geer moraines and the Kumla esker indicates that the studied area was also
12 163 occupied by a highly indented calving bay during ice retreat.

164 **Materials and methods**

165 The topographical data used in this paper is the LiDAR derived digital elevation model
166 (DEM) supplied by the Swedish national mapping agency (Lantmäteriet;
167 <http://www.lantmateriet.se>). This arrives to the end user with an average vertical accuracy of
168 ~0.1 m and a pixel resolution of 2 m. The data is pre-processed to remove both vegetation
169 cover and urban areas down to ‘true’ ground level. The technical details for this height model
170 can be found in Dowling et al. (2013). Data handling was carried out in ArcGIS[®] 10.0 and
171 Matlab[®] R2014^a.

172 Mapping of the landforms was manually carried out on hill-shade models illuminated from a
173 variety of angles. The small scale drumlins are only visible with x5 height exaggeration
174 applied and the careful manipulation of the angle of illumination. Typically the best angle of
175 illumination with which to see these features is either from 120° or 250°. Switching between
176 these angles and 90° reveals the small, shallow, drumlins. The mapping itself was carried out
177 as part of the work outlined in Dowling et al. (2015), and the drumlins are part of that larger
178 dataset. Height was extracted using the method of Spagnolo et al. (2012), whilst length and
179 width were extracted using minimum bounding geometry (Napieralski and Nalepa, 2010).

180 **Results**

181 *Landform descriptions*

182 The studied Kumla–Örebro area (~13 by 8 km), depicted in Figs. 3 and 4, contains
183 streamlined bedforms (drumlins) in two size ranges (Fig. 4). The larger features are typically

1
2
3 184 430-2200 m long, 110-400 m wide, and 8-15 m high (Table 1) and, when compared to the
4
5 185 metrics of global datasets (Clark et al., 2009; Spagnolo et al., 2012), could be considered
6
7 186 ‘classic’ drumlins. These drumlins are part of the general streamlined flow set of the wider
8
9 187 region of the Närke plain and are aligned approximately north to south (Möller and Dowling,
10
11 188 2016). The second size range of streamlined bedforms is an order of magnitude smaller and is
12
13 189 distributed at an angle to these larger features. Perpendicularly overlaid on these small-scale
14
15 190 drumlins are suites of De Geer moraines (Fig. 4). The distribution of, and relations between,
16
17 191 these geomorphic forms are further detailed in our LiDAR-derived DEMs over three chosen
18
19 192 smaller type areas, the Härminge and Brickebacken sub-areas, to the east of the Kumla esker
20
21 193 (Figs. 5 and 7), and the Stora Ulvgryta sub-area, to the west of said esker (Fig. 8).

22
23 194 The features in the Härminge sub-area (Fig. 5) clearly indicate the calving-bay orientation
24
25 195 relationship between small-scale drumlins, De Geer moraines and the esker. The area (~7
26
27 196 km²) hosts small-scale drumlins ($n = 48$) that are 41-245 m long and 10-71 m wide, with a
28
29 197 P_{10} - P_{90} height of 0.4-1.8 m (Table 1). Drumlin axes are orientated ~35/215°. Draped over the
30
31 198 drumlins is a dense set of De Geer moraines (Fig. 6), all trending ~305/125°. These are thus
32
33 199 perpendicular to the Härminge small-scale drumlins, but skewed relative to the larger
34
35 200 drumlins (e.g. right-hand side on Fig. 5). The De Geer moraines in the Härminge area (Fig. 5)
36
37 201 measure 25-832 m in length, 10-21 m in width and 2-3 m in height. The Härminge small-scale
38
39 202 drumlins and the De Geer moraines associated with them are thus at an angle of ~38° to the
40
41 203 north-south esker trend. It should be noted that for both the De Geer moraines and especially
42
43 204 for the small-scale drumlins in this sub-area there is the potential for a shrouding effect
44
45 205 (Finlayson, 2014; Spagnolo et al., 2014) when surrounded by on-lapping glacial/postglacial
46
47 206 aquatic sediments (silt and clay; Fig. 3). In some areas with deep successions of aquatic
48
49 207 sediments and/or organic deposits this shrouding effect can be several meters (e.g., Möller
50
51 208 and Dowling (2016) for the nearby Hackvad drumlin field); this can come close to completely
52
53 209 ‘drowning’ smaller geomorphic features.

54
55 210 The Brickebacken sub-area (Fig. 7) is due north of the Härminge sub-area (Fig. 4), covering
56
57 211 about 24 km². Small-scale drumlins in this set ($n = 155$) are 68-176 m long, 17-57 m wide and
58
59 212 1.5-2.3 m high (P_{10} - P_{90} values). Drumlin axes are orientated ~35/215°, i.e. the same direction
60
213 as at Härminge, but these features are here more densely packed. Bedrock outcrops associated
214
215 214 with the drumlins are often detectable from the Quaternary mapping and from visual
216
217 215 inspection of the hill shade model, suggesting that mapped drumlins are of the rock-cored
218
219 216 type. As at Härminge, the drumlins are superimposed by De Geer moraines that trend

1
2
3 217 ~305/125°, although some of the moraines start to shift towards a ~290/105° alignment
4
5 218 towards the eastern margin of the demarcated area. The De Geer moraines are 12-264 m long,
6
7 219 ~20-21 m wide and ~1-2 m high. The shrouding effect is likely minimal here, as the features
8
9 220 are located on a slightly elevated till plain with no subaquatic sediments preserved between
10
11 221 moraine ridges. However, just outside of our mapped subarea there are features drowned in
12
13 222 subaquatic fine-grained sediment which are now only visible as crop marks in aerial photos
14
15 223 and as faint shadows in the hillshade models.

16
17 224 The Stora Ulvgryta sub-area (Fig. 8) is situated west of the Brickebacken area, covering about
18
19 225 30 km². Importantly, it is located on the western side of the Kumla esker (Fig. 4). The small-
20
21 226 scale drumlins in this set ($n = 54$) have the same general pattern of morphometrics as the sub-
22
23 227 areas on the eastern side of the esker. The drumlins are 65-241 m long, 22-70 m wide and 1-3
24
25 228 m high (P_{10} - P_{90} values) and have axes orientated ~350/170°. Rock outcrops associated with
26
27 229 the mapped drumlins are often detectable from the Quaternary mapping and the hill shade
28
29 230 model. The drumlins are sparsely distributed and overlain by a small number of De Geer
30
31 231 moraines that are 55-183 m long, ~14-21 m wide and ~0.5-1 m high, trending ~70/250°.

32
33 232 Taken together, the orientation of the small drumlins and their associated De Geer moraines
34
35 233 on opposite sides of the Kumla esker provide strong evidence of the geometric development
36
37 234 of the calving bay and ice margin retreat in the Kumla-Örebro region, as well as indicating the
38
39 235 local, late-stage ice flow direction.

236 **Discussion**

237 *Advantages of using LiDAR terrain data*

238 Without high resolution LiDAR it would be impossible to detect the small-scale drumlin
239 features described here. Their small size, in particular their shallow height, makes their
240 detection in the field or from traditional aerial photograph mapping very difficult. This is
241 especially the case when located under forest cover, making the capability of LiDAR to 'look
242 through' vegetation as important as a high spatial resolution for their detection. The work
243 done here shows the ability of high resolution LiDAR datasets to create detailed
244 reconstructions of palaeo-landform assemblages, combining both previously identified
245 landforms and newly identified relationships between these landforms with newly discovered
246 features. Furthermore, the mapping of De Geer moraines with LiDAR-based DEM's results in
247 much denser and detailed patterns as compared to previous ground- and aerial photograph-

1
2
3 248 based mapping (see also Bouvier et al., 2015). This enhancement is very evident when
4 249 comparing their mapped distributions in Fig. 3B versus Figs. 4, 5, 7 and 8. This further
5
6 250 strengthens any assessment of probable calving bay configuration.
7

8
9 251 *Palaeo-calving bay formation*

10
11 252 The pattern and direction of near-to-esker De Geer moraines provide evidence that the
12
13 253 receding ice margin formed pronounced indentions – a calving bay – around the Kumla esker
14
15 254 that formed transgressively backwards at the subaqueous outlet of the subglacial drainage at
16
17 255 deglaciation of the area. As the bay retreated northwards it also opened out, i.e. the angle
18
19 256 between the ice-front and the esker/drainage outlet increased as the margin moved north (see
20
21 257 Fig. 9 and mapping in Fig. 4).

22
23 258 The retreat of water-terminating ice margins is due to a balance of and feedbacks between
24
25 259 calving, topography and atmospheric warming (e.g. Venteris, 1999; Cook et al., 2005; Benn et
26
27 260 al., 2007a). Localized areas with higher ice loss over longer or shorter time periods, caused by
28
29 261 preferential calving at an active sub-surface drainage outlet (Benn et al., 2007b), might thus
30
31 262 result in concave calving bays. According to Benn and Evans (2010) this is most likely the
32
33 263 result of longitudinal extension occurring in conjunction with simple shear at the ice margin.
34
35 264 The effect of this is to generate distinctive crevasse patterns along which the enhanced calving
36
37 265 occurs, forming the concave planform of calving bays near eskers. An important factor in a
38
39 266 given calving rate is water depth (Benn et al., 2007a); postulated palaeo calving bays across
40
41 267 the subaqueously deglaciated south-central part of Sweden (Fig. 1) were evidently tied to the
42
43 268 positions of the larger eskers of this area. This might indicate the importance of this factor: the
44
45 269 eskers are usually situated in the lowermost positions of this once submerged landscape.

46
47 270 However, water depth differences along the receding ice margin were not that large. Possibly
48
49 271 more important in controlling calving rate was the *per se* existence of the subglacial drainage
50
51 272 conduits, marked in their deglacial positions by the resulting eskers. Melting of the ice above
52
53 273 these conduits and in their immediate surroundings would thin the ice, reduce basal effective
54
55 274 stresses and thus basal drag, introduce positive feedback into dynamic thinning and
56
57 275 propagation of deep surficial crevasses up-glacier, thus resulting in localized increases in
58
59 276 calving rate (e.g. Benn et al., 2007; Benn and Evans, 2010). A continuous fast differential ice
60
277 loss close to the eskers as compared to the areas between the eskers would, however,
278 theoretically mean that the calving bays would get progressively deeper with time.

1
2
3 279 When scrutinizing the maps of calving bay configurations as suggested from constructed varve
4 280 isochrones, e.g. Strömberg (1989), see Fig. 2B, or further north in the county of Dalarna
5 281 (Fromm, 1991) with very deep calving bays, it is evident that there was a tendency for calving
6 282 bays to grow progressively deeper with time, but only over portions of their recessional paths.
7
8 283 This suggests that the calving rate in the calving bays was larger than the regional ice recession
9 284 rate only over shorter periods of time, i.e. intermittent periods of fast calving. This was
10 285 followed by a reduction in the rate of ice loss back to the typical regional ice recession rate
11 286 with the generated calving bay configuration moving back into a more typical marginal
12 287 alignment.

13
14
15
16
17
18
19 288 *Location of drumlin formation and ice flow adjustment*

20
21 289 Based on their perpendicular relationship with the ice-marginal De Geer moraine ridges we
22 290 argue that the orientation of the small-scale drumlins in the Kumla-Örebro area, as depicted
23 291 in Fig. 4, reflects the direction of ice flow near the Kumla esker at a late stage of deglaciation.
24
25 292 The smaller-scale drumlins formed within a near-marginal area where the regional north to
26 293 south-directed ice flow had shifted as a response to the formation of an indented calving bay
27 294 (Fig. 9). The orientation of De Geer moraine ridges changes slightly throughout the study area
28 295 as the ice margin geometry was modified during retreat. However, these differences are too
29 296 small to be able to associate individual drumlins to specific De Geer ridges. Thus it is not
30 297 possible to establish whether an individual drumlin formed while the margin was only a few
31 298 hundred metres away in distal direction or some kilometres, as its orientation remains roughly
32 299 perpendicular to that of most De Geer ridges. Yet, since the orientation of the latter shifts
33 300 abruptly on either side of the Kumla-esker it is almost certain that the maximum distance
34 301 between the forming drumlins and the ice margin is represented by the distance to the esker.
35 302 This has to be measured along the once existing ice flowlines as evidenced by the small-scale
36 303 drumlins, and can be practically obtained by simply projecting down-flow the drumlin long
37 304 axis until this intercepts the esker. In the other direction a hypothetical flow line would
38 305 gradually fall into the primary N-S directed flow lines that are not influenced by the calving
39 306 bay configuration. The measured distances of this varies from 1 km in the south of the study
40 307 area (near the 'x' of the transect marked in Fig. 4), to 7.7 km, further north.

41
42
43
44
45
46
47
48
49
50
51
52
53 308 The concept of retreating margins controlling drumlin orientations has previously been
54 309 discussed by Mooers (1989). In a time-transgressive model of drumlin formation located
55 310 under the Rainy and Superior lobes of the Laurentide ice sheet, it was shown that the trend of
56
57
58
59
60

1
2
3 311 drumlin axes was primarily set by a retreating ice margin. However, Mooers' model only
4 312 located this within a distance of 20-30 km of said ice margin, rather than the more proximal
5 313 distance of approximately 1-7.7 km that we report here.

6
7
8 314 *Formation time*

9
10
11 315 Based on our proposed model of *where* the small-scale drumlins formed in relation to the ice
12 316 margin it is possible to calculate the time frame over which individual/adjacent near-marginal
13 317 drumlins were formed. This is a function of the time period over which the calving bay-
14 318 adjusted ice flow was operating over the ice-bed interface of the area in question. Therefore it
15 319 is possible to infer the maximum formation time from a known local ice recession rate.
16 320 Ideally we would be able to use the De Geer moraine ridges to do this, and this was the
17 321 original idea by De Geer (1989), i.e. that the ridges had geochronological significance in that
18 322 they were formed annually. This has also lately been suggested from a study of Swedish De
19 323 Geer moraines by Bouvier et al. (2015). However, such annuality has been rejected by, e.g.,
20 324 Hoppe (1959) and Strömberg (1965), as well as by Lindén and Möller (2005), who all argued
21 325 that multiple moraines could form within the same year. We thus argue that we cannot use the
22 326 mean distance between De Geer moraines in the Kumla-Örebro area as a reliable
23 327 chronometer.

24
25
26 328 However, it is possible to use the Swedish varve chronology to gain an appreciation of local
27 329 deglaciation time and the time frame over which the small-scale drumlins were formed. The
28 330 close to parallel and regularly spaced isochrones between -1200 and -900 over and north of
29 331 Stockholm (Fig. 1) suggest that these isochrones can, with a relatively high confidence, be
30 332 transferred laterally west-southwest-wards. This allows us to infer that the whole Kumla-
31 333 Örebro area was deglaciated between varve isochrones -1200 and -1100, i.e. in less than 100
32 334 years. This is then an absolute maximum time period for all the mapped small-scale drumlins
33 335 to form as their formation must have taken place during the passage of the Kumla-esker
34 336 calving bay, with their orientation showing an adjustment to this ice marginal configuration.
35 337 The 20 varve-year isochrones of Strömberg (1989) between years -1200/-1100 give an annual
36 338 mean steady state recession rate of ~220 m/yr. Although the recession rate value could have
37 339 varied locally along the gradually receding calving bay margin due to differences in calving
38 340 rates/events, and therefore not be a steady-state retreat, we argue that it can be used as a good
39 341 average for the northwards propagation of the calving bay margin.

1
2
3 342 With this assumption in place the transect X-Y in Fig. 4 with a length of 7.7 km in the
4
5 343 Härminge and Brickebacken sub-areas, was deglaciated within ~30-35 years from the first
6
7 344 mapped De Geer moraine to the last. This was then a period that also time-transgressively
8
9 345 sustained the NE to SW-directed ice flow towards the eastern flank of the calving bay at
10
11 346 which point the smaller-scale drumlins were formed. A formation time of only a few decades
12
13 347 is further reinforced by the situation verified in the Stora Ulvgryta sub-area, on the opposite
14
15 348 side of the Kumla esker (Fig. 8). A SE-directed, 5.3 km long, transect across De Geer
16
17 349 moraines draping the Stora Ulvgryta drumlins gives, under the same assumptions as above, a
18
19 350 deglaciation time of the whole transect of ~24 years. The slight chronological difference
20
21 351 between the two sides of the esker also demonstrates that De Geer moraines are not a reliable
22
23 352 chronometer for ice retreat rate. There are sections along the X-Y transect (Fig. 4) over which
24
25 353 there are very small spaces between the ridges (12 moraines over 1000 m; i.e. a mean spacing
26
27 354 of 83 m) which means that the number of ridges formed could have been as high as 2-3 ridges
28
29 355 per year or even more over shorter steps of ice margin retreat.

30
31 356 Our calculated period for the formation of the small-scale drumlins is a maximum time
32
33 357 period, referring as discussed above to the total deglacial age span with a sustained ice flow
34
35 358 direction from NE and NW on either side of the Kumla esker. Should the minimum distance
36
37 359 to the esker of 1 km, verified for some of the drumlins, be taken into consideration, the
38
39 360 formation time of these features is reduced to only 5 years. This is compatible with recent
40
41 361 observations such as the repeat seismic and radar investigations under the Antarctic Rutford
42
43 362 Ice Stream, which revealed a 10 m high and 100 m wide streamlined bedform
44
45 363 forming/evolving within a period of only 7 years (Smith et al., 2007; King et al., 2009). In
46
47 364 agreement with these results there is also a recent study on the formation time of drumlins at
48
49 365 Fláajökull on Iceland (Jónsson et al., in press), similar in size to the ones analysed here, with a
50
51 366 suggested ~29 year formation time-frame. This is particularly interesting as a modern
52
53 367 example in a non-surge setting with a well-controlled formation time. The calculated drumlin
54
55 368 formation time of our study also fits within the broad time frame for drumlin formation
56
57 369 calculated by Rose (1989) of 8-292 years, falling within the lower end of that range. The
58
59 370 calculations by Rose (1989) build on sediment transfer rates applied to volume of tills in their
60
371 investigated drumlins; though an interesting approach this is hard to apply to the drumlins
372 described here. This is because the transfer rate of till for our region is largely unknown and
373 the volume of till in the drumlins is hard to evaluate as these features are likely rock cored, as
374 drumlins predominantly are in southern Sweden (Dowling et al., 2015).

1
2
3 375 In summary, the small-scale drumlins identified here formed ~1-7.7 km behind a retreating
4 376 calving bay ice margin and over formation periods of 5 to 35 years. The larger drumlins of the
5 377 area, which are an order of magnitude larger than the small-sized features and which are
6 378 parallel to the regional north to south-directed ice flow, should have formed over a much
7
8 379 longer period. Our reconstructions are further supported by the following lines of evidence:

9
10
11 380 (i) Smaller drumlins over-print the larger drumlins. The survival of the larger drumlins,
12 381 despite the near ice-marginal change in flow direction and subsequent sediment reorganisation
13 382 into the smaller drumlins shown here suggests that the duration of the flow event that created
14 383 the small-scale drumlins was not long enough, or lacked the erosive/deformative capacity, to
15 384 alter the orientation of the large drumlins.

16
17
18 385 (ii) The small-scale drumlins are only present in connection to closely spaced De Geer
19 386 moraines. This indicates that the small-scale drumlins only formed in places where the ice
20 387 margin had a quasi-stable ice retreat rate without large calving events that could have
21 388 generated large frontal retreats greater than several hundreds of metres.

22 23 24 25 26 27 28 29 389 **Conclusions**

30
31
32 390 We have found that small-scale drumlins in the Kumla-Örebro area are aligned – and thus
33 391 formed – parallel to flow lines that were adjusted to the configuration of calving embayments
34 392 in the receding ice margin at the last deglaciation. These embayments were located close to
35 393 the position of where larger eskers formed and were the product of enhanced calving at the
36 394 subaqueous outlets of the subglacial melt-water drainage. Furthermore, the area/calving
37 395 margin under which our mapped small-size drumlins formed was likely deglaciated over a
38 396 period of ~25-35 years, suggesting a maximum timeframe for their formation. To summarise,
39 397 the key findings of this paper are:

- 40
41
42
43
44
45
46 398 • Enhanced calving processes around the subaqueous outlets of well-developed
47 399 subglacial drainage networks caused marginal ice flow direction to converge towards
48 400 the outlet/resulting esker. The result of this was the formation of calving bays and an
49 401 altered near-marginal ice flow direction. This is demonstrated by the geometric
50 402 relationship of drumlins, De Geer moraines and the Kumla esker in the studied area.
- 51
52
53
54
55
56
57
58
59
60

- 1
2
3 403 • Mapped small-scale drumlins can form behind calving bays in response to the change
4 404 in flow direction. This has been verified in the Kumla-Örebro region where the
5 405 drumlins must have formed within c. 1-8 km of the active glacial margin.
6
7
8 406 • Our studies suggest that drumlins of the size described can form under major ice-
9 407 sheets over very short time periods, 5-35 years.

408 Acknowledgements

409 The work presented here is part of a larger project (with P. Möller as PI) on formation of
410 streamlined terrain over south Sweden which, together with the papers by Dowling et al.
411 (2013), Dowling et al. (2015), Möller and Dowling (2015), Möller and Dowling (2016) and
412 Dowling et al. (2016) lead to, and are summarized in, the PhD thesis by Dowling (2016). The
413 LiDAR data used in this work is the property of Lantmäteriet (<http://www.lantmateriet.se>) and
414 is done so under agreement number: i2014 / 00579. Comments by JQS reviewers Julia
415 Wellner, Clas Hättestrand and an anonymous reviewer greatly improved the focus of the paper.

416 References

- 417 Bannerjee I, McDonald, BC. 1975. Nature of esker sedimentation. *In* Jopling, AV, McDonald,
418 BC. (eds.): Glaciofluvial and glaciomarine sedimentation. *SEPM Spec. Publ.* **23**:
419 132-154.
420 Benn DI, Evans DJA. 2010. *Glaciers and Glaciation*. Hodder Education, Euston Road,
421 London, UK: 802 p.
422 Benn DI, Hulton NRJ, Mottram RH. 2007^a. 'Calving laws, 'sliding laws' and the stability of
423 tidewater glaciers. *Annals of Glaciology* **46**: 123-130.
424 Benn DI, Warren CR, Mottram RH. 2007^b Calving processes and the dynamics of calving
425 glaciers. *Earth-Science Reviews* **82**: 143-179.
426 Bergdahl A. 1959. Glaciofluvial estuaries on the Närke plain. *Svensk Geografisk Årsbok* **35**:
427 47-70.
428 Bergdahl A. 1961. Det glaciala landskapet. Kumlabygden, Forntid - Nutid – Framtid, del 1,
429 *Berg, jord och skogar*, 203-326. Kumla stad och Kumla Landskommun.
430 Bergdahl A. 1965. Isvikar och åsar i Kumla-Hallsbergsområdet. *Svensk Geografisk Årsbok*
431 **41**: 50-63.

- 1
2
3 432 Björck J, Possnert G, Schoning K. 2001. Early Holocene deglaciation chronology in
4 433 Västergötland and Närke, southern Sweden – biostratigraphy, clay varve, ¹⁴C and
5 434 calendar year chronology. *Quaternary Science Reviews* **20**: 1309-1326.
6
7
8 435 Björck S. 1995: A review of the history of the Baltic Sea, 13.0-8.0 ka BP. *Quaternary*
9 436 *International* **27**: 19-40.
10
11 437 Bouvier V, Johnsson M, Pässe T. 2015. Distribution, genesis and annual-origin of De Geer
12 438 moraines in Sweden: insights revealed by LiDAR. *GFF* **137**: 319-333.
13
14 439 Brunnberg L. 1995. Clay-varve chronology and deglaciation during the Younger Dryas and
15 440 Pre-boreal in easternmost part of the Middle Swedish Ice Marginal Zone. *Quaternaria*
16 441 *Series A:2 Thesis*: 95 pp.
17
18 442 Cato I. 1985. The definitive connection of the Swedish geochronological time scale with the
19 443 present, and the new date of the zero year in Döviken, northern Sweden. *Boreas* **14**:
20 444 117-122.
21
22 445 Cato I. 1987. On the definitive connection to the Swedish Time Scale with the present.
23 446 *Sveriges Geologiska Undersökning Ca* **68**: 55 pp.
24
25 447 Clark, CD. 2010. Emergent drumlins and their clones: from dilatancy to flow instabilities.
26 448 *Journal of Glaciology* **51**: 1011-1025.
27
28 449 Clark, CD., Hughes, AL., Greenwood, SL., Spagnolo, M. and Ng, FS., 2009. Size and shape
29 450 characteristics of drumlins, derived from a large sample, and associated scaling laws.
30 451 *Quaternary Science Reviews*, **28**(7), pp.677-692.
31
32 452 Cook AG, Fox AJ, Vaughan DG, Ferrigno JG. 2005 Retreating glacier fronts on the Antarctic
33 453 Peninsula over the past half-century. *Science* **22**: 541-544.
34
35 454 De Geer G. 1989. Ändmoränerna i trakten mellan Spånga och Sundbyberg. *GFF* **11**: 395-396.
36 455 De Geer G. 1897. Om rullstensåsars bildningssätt. *Sveriges Geologiska Undersökning C* **197**:
37 456 25 pp. De Geer, G. 1940. Geochronologica Suecica Principles. *Kungliga Svenska*
38 457 *Vetenskapsakademiens handlingar 3dje Serien Bd* **18(6)**: 367 pp.
39
40 458 Dowling TPF. 2016. The drumlin problem – streamlined subglacial bedforms in southern
41 459 Sweden. *LUNDQUA Thesis* **80**: 1-32. Department of Quaternary Sciences/Department
42 460 of Geology, Lund University. (<https://lup.lub.lu.se/search/publication/8569667>)
43
44 461 Dowling TPF, Alexanderson H, Möller P. 2013. The new high-resolution LiDAR digital
45 462 height model ('Ny Nationell Höjdmodell') and its application to Swedish Quaternary
46 463 geomorphology. *GFF* **135**: 145-151.
47
48
49
50
51
52
53
54
55
56
57
58
59
60

- 1
2
3 464 Dowling TPF, Spagnolo M, Möller P. 2015. Morphometry and core type of streamlined
4 465 bedforms in southern Sweden from high resolution LiDAR. *Geomorphology* **236**: 54-
5 466 63.
6
7
8 467 Dowling TPF, Möller P, Greenwood S, Spagnolo M, Åkesson M, Hughes A, Frasier S, Clark
9 468 C. 2016. The extent to which geological factors influence the shape of streamlined
10 469 subglacial landforms. Submitted to *Geomorphology*. In Dowling TPF, The drumlin
11 470 problem – streamlined subglacial bedforms in southern Sweden. *LUNDQUA Thesis* **80**:
12 471 57-78. Department of Quaternary Sciences/Department of Geology, Lund University.
13 472 (<https://lup.lub.lu.se/search/publication/8569667>)
14
15
16
17
18 473 Ericsson B. 1979. Description to the Quaternary map Karlskoga SO. *Sveriges Geologiska*
19 474 *Undersökning Ae* **37**: 108 pp.
20
21 475 Fredén C. (ed.), 2009. *Berg och jord, Sveriges Nationalatlas* (4th ed.). Nordstedts Kartor AB,
22 476 Bromma, Sweden. 208 pp. ISBN 978-91-87760-56-3.
23
24 477 Fromm E. 1972. Description of the Geological map Örebro SV. *Sveriges Geologiska*
25 478 *Undersökning Ae* **5**: 100 pp.
26
27
28 479 Fromm E. 1991. Varve chronology and deglaciation in south-eastern Dalarna, central Sweden.
29 480 *Sveriges Geologiska Undersökning Ca* **77**: 49 pp.
30
31 481 Frödin G. 1916. Über einige spätglaziale Kalbungsbukten und fluvioglaziale Estuarien im
32 482 mittleren Schweden. *Bulletin Geologiska Institutionen, Upsala* **15**: 149-174.
33
34 483 Glückert G. 1973. Two large drumlin fields in central Finland. *Fennia* **120**: 37 pp.
35
36 484 Glückert G. 1987. The drumlins of central Finland. Pp. 291-307 in Menzies, J. & Rose, J.
37 485 (eds.): *Drumlin Symposium*. A. A. Balkema. 360 pp.
38
39 486 Hoppe G. 1948. Isrecessionen från Norrbottens Kustland i belysningen av de glaciala
40 487 formelementen. *Geographica* **20**: 112 pp. (Uppsala University, Department of
41 488 Geography)
42
43
44 489 Hoppe G. 1957. Problems of glacial geomorphology and the ice age. *Geografiska Annaler* **39**:
45 490 1-18.
46
47
48 491 Hoppe G. 1959. Glacial morphology and inland ice recession in northern Sweden.
49 492 *Geografiska Annaler* **41**: 193–212.
50
51 493 Hättestrand C, Götz S, Näslund JO, Fabel D, Stroeven AP. 2004. Drumlin formation time:
52 494 evidence from northern and central Sweden. *Geografiska Annaler: Series A, Physical*
53 495 *Geography* **86**, 155-167.
54
55
56
57
58
59
60

- 1
2
3 496 Johnson MD, Schomacker A, Benediktsson ÍÖ, Geiger AJ, Ferguson A, Ingólfsson Ó. 2010.
4 497 Active drumlin field revealed at the margin of Múlajökull, Iceland: a surge-type
5 498 glacier. *Geology* **38(10)**: 943-6.
6
7 499 Jónsson SA, Benediktsson ÍÖ, Ingólfsson Ó, Schomacker A, Bergsdóttir HL, Jacobson jr WR,
8 500 Linderson H. (*in press*). Submarginal drumlin formation and late Holocene history of
9 501 Fláajökull, southeast Iceland. *Annals of Glaciology*
10
11 502 King, EC, Hindmarsh, RC, Stokes, C. 2009. Formation of mega-scale glacial lineations
12 503 observed beneath a West Antarctic ice stream. *Nature Geoscience* **2**, 585-588.
13
14 504 Kranck, K. 1973. Flocculation of suspended sediment in the sea. *Nature* **246**, 348-350.
15
16 505 Lamsters K, Zelčs V. 2015. Subglacial landforms of the Zemgale Ice Lobe, south-eastern
17 506 Baltic. *Quaternary International* **386**: 42-54
18
19 507 Lindén M, Möller P. 2005. Marginal formation of De Geer moraines and their implications to
20 508 the dynamics of grounding-line recession. *Journal of Quaternary Science* **20**: 113-133.
21
22 509 Lundqvist J. 2009. Weichsel-istidens huvudfas. In *Berg och jord, Sveriges Nationalatlas*,
23 510 Fredén C. (ed.). Nordstedts Kartor AB, Bromma, Sweden. (4th ed.): 124-135. ISBN
24 511 978-91-87760-56-3.
25
26 512 Magnusson E. 1984. Description to the Quaternary map Västerås SO. *Sveriges Geologiska*
27 513 *Undersökning A* **64**: 76 pp.
28
29 514 Mangerud J, Gyllenkretz R, Lohne Ø, Svendsen JI. 2011. Glacial history of Norway. In
30 515 *Quaternary Glaciations - Extent and Chronology - a closer look*, Ehlers J., Gibbard
31 516 PL, Hughes, PH (eds.), *Developments in Quaternary Science* **15**: 279-298. Elsevier.
32
33 517 Menzies J. 1979. A review on the literature on the formation and location of drumlins. *Earth*
34 518 *Science Reviews* **14**: 315-359.
35
36 519 Mooers HD. 1989. Drumlin formation: a time transgressive model. *Boreas* **18**, 99-107.
37
38 520 Möller P, Dowling TPF. 2016: Streamlined subglacial bedforms on the Närke plain, south-
39 521 central Sweden – areal distribution, morphometrics, internal architecture and
40 522 formation. *Quaternary Science Reviews* **X**: xx-xx (accepted).
41
42 523 Napieralski J, Nalepa N. 2010. The application of control charts to determine the effect of
43 524 grid cell size on landform morphometry. *Computers & Geosciences* **36**: 222-230.
44
45 525 Nilsson E. 1968. Södra Sveriges senkvartära historia. Geokronologi, issjöar och landhöjning.
46 526 *Kungliga Svenska Vetenskapsakademins Handlingar*, **4th ser., vol. 12**: 117 pp.
47
48 527 Raukas A, Tavast E. 1994. Drumlin location as a response to bedrock topography on the
49 528 southeastern slope of the Fennoscandian Shield. *Sedimentary Geology* **91**: 373-382.
50
51
52
53
54
55
56
57
58
59
60

- 1
2
3 529 Rose, J. 1989. Glacier stress patterns and sediment transfer associated with the formation of
4 530 superimposed flutes. *Sedimentary Geology* **62**: 151-176.
- 5
6 531 Skei JM, Syvitski JPM. 2013. Natural flocculation of mineral particles in seawater – influence
7 532 on mine tailing sea disposal and particle dispersal. *Mineralproduktion* **3**:A1-A10.
- 8
9 533 Smith AM, Murray T, Nicholls KW, Makinson K, Aðalgeirsdóttir G, Behar AE, Vaughan
10 534 DG. 2007. Rapid erosion, drumlin formation, and changing hydrology beneath an
11 535 Antarctic ice stream. *Geology* **35**: 127-130.
- 12
13 536 Spagnolo M, Clark CD, Hughes ALC. 2012. Drumlin relief. *Geomorphology* **153-154**: 179-
14 537 191.
- 15
16 538 Stokes CR, Fowler AC, Clark CD, Hindmarsh RC, Spagnolo M. 2013. The instability theory
17 539 of drumlin formation and its explanation of their varied composition and internal
18 540 structure. *Quaternary Science Reviews* **62**, 77-96.
- 19
20 541 Stokes CR, Spagnolo M, Clark CD. 2011. The composition and internal structure of drumlins:
21 542 complexity, commonality, and implications for a unifying theory of their formation.
22 543 *Earth-Science Reviews* **107**: 398-422.
- 23
24 544 Stroeve AP, Heyman J, Fabel D, Björck S, Caffee MW, Fredin O, Harbor JM. 2015. A new
25 545 Scandinavian reference ¹⁰Be production rate. *Quaternary Geochronology* **29**:104-115.
- 26
27 546 Stroeve AP, Hättestrand C, Kleman J, Heyman J, Fabel D, Fredin O, Goodfellow BW,
28 547 Harbor JM, Jansen JD, Olsen L, Caffee MW, Fink D, Lundqvist J, Rosqvist GC,
29 548 Strömberg B, Jansson KN. 2015. Deglaciation of Fennoscandia. *Quaternary Science*
30 549 *Reviews* **X**: xx-xx (in press).
- 31
32 550 Strömberg B. 1965. Mapping and geochronological investigations in some moraine areas of
33 551 south-central Sweden. *Geografiska Annaler* **47A**: 73-82.
- 34
35 552 Strömberg B. 1981. Calving bays, striae and moraines at Gysinge-Hedesunda, central
36 553 Sweden. *Geografiska Annaler* **63A**: 149-154.
- 37
38 554 Strömberg B. 1989. Late Weichselian deglaciation and clay varve chronology in east-central
39 555 Sweden. *Sveriges Geologiska Undersökning* **Ca 73**: 70 pp.
- 40
41 556 Strömberg B. 1994. Younger Dryas deglaciation at Mt Billingen, and clay varve dating of the
42 557 Younger Dryas/Preboreal transition. *Boreas* **23**:177-193.
- 43
44 558 Svendsen JI, Alexanderson H, Astakhov VI, Demidov I, Dowdeswell JA, Funder S, Gataulin V,
45 559 Henriksen M, Hjort C, Houmark-Nielsen M, Hubberten HW, Ingólfsson Ó, Jakobsson
46 560 M. Kjær KH, Larsen E, Lunkka JP, Lyså A, Mangerud J, Matiushkov A, Murray A,
47 561 Möller P, Niessen F, Nikolskaya O, Polyak L, Saarnisto M, Siegert C, Siegert MJ,

- 1
2
3 562 Spielhagen RF, Stein R. 2004. The Late Weichselian Quaternary ice sheet history of
4 563 northern Eurasia. *Quaternary Science Review* **23**: 1229–1271.
5
6 564 Warren WP, Ashley GM. 1994. Origins of the ice-contact stratified ridges (eskers) of Ireland.
7
8 565 *Journal of Sedimentary Research* **A64**: 433-449.
9
10 566 Wellner JS, Lowe AL, Shipp SS, Anderson JB. 2001. Distribution of glacial geomorphic
11 567 features on the Antarctic continental shelf and correlation with substrate: implications
12 568 for ice behavior. *Journal of Glaciology* **47**: 397-411.
13
14 569 Venteris, E.R. 1999 Rapid tidewater glacier retreat: a comparison between Columbia Glacier,
15 570 Alaska and Patagonian calving glaciers. *Global and Planetary Change* **22**: 131-138.
16
17 571
18
19
20
21
22
23
24
25
26
27
28
29
30
31
32
33
34
35
36
37
38
39
40
41
42
43
44
45
46
47
48
49
50
51
52
53
54
55
56
57
58
59
60

572 **Captions and Tables**

573

	<i>n</i>	<i>Mean Height</i>	<i>Height P₁₀</i>	<i>Height P₉₀</i>	<i>Mean Length</i>	<i>Length P₁₀</i>	<i>Length P₉₀</i>	<i>Mean Width</i>	<i>Width P₁₀</i>	<i>Width P₉₀</i>	<i>Mean Orientation</i>
<i>Area 1</i>	48	0.9	0.4	1.8	113.5	64.8	188.8	31	15.3	57.6	35-215
<i>Area 2</i>	155	1.5	0.8	2.3	112.7	68.4	175.3	33	17.7	56.4	30-210
<i>Area 3</i>	54	1.8	1	3	117.4	65	240.8	40.4	22.2	70.8	210-30

574

575 Table 1. Summary statistics for flow set morphometrics. All values are in meters and rounded
 576 to 1 decimal point. Mean orientation is given to the nearest whole degree, the values
 577 representing the orientation of the a-axis, with the upstream polarity given first.

578 Fig. 1. (A) Overview of NW Europe. Red dashed line = proposed Fennoscandian Ice Sheet
 579 margin to the west/south at LGM (Svendsen et al., 2004); blue dashed line = the Younger
 580 Dryas Ice Marginal Zone (Mangerud et al., 2011). (B) Map of southern Sweden (for location,
 581 white box in (A)), showing areas above and below the highest shoreline (marine limit in the
 582 west), and altitude of the highest shoreline at deglaciation. The highest shoreline east of
 583 Billingen is the shore altitude for the Baltic Ice Lake prior to its 2nd drainage at retreat from
 584 Billingen after the Younger Dryas advance, while highest shoreline isobases north thereof
 585 were formed in the following Baltic Basin stages Yoldia Sea and Ancylus Lake (Björck,
 586 1995), following the northwards receding ice margin. Inferred ice-marginal positions during
 587 the Younger Dryas are according to Lundqvist (2009). Deglacial varve isochrones are
 588 transferred from Brunberg (1995) (south of Stockholm), Strömberg (1994) (Lake Vänern-
 589 Askersund) and Strömberg (1989) (north of Stockholm). Base map compiled from the
 590 Swedish National Atlas (Fredén, 2009). Red box marks the investigated area between Örebro
 591 and Kumla (Fig. 3) and orange boxes mark the positions of Figs. 2A and 2B. Typical ice flow
 592 for the local area was north-south.

593 Fig. 2. Examples of reconstructed calving bays around some of the larger eskers north of
 594 Lake Mälaren, south-central Sweden (Fig. 1B), based on varved clay measurements (redrawn
 595 from Plates 2 and 3 in Strömberg (1989)). Eskers are shown in green, striae outcrop locations
 596 are marked with a red with the direction indicated by the red line and the black lines indicate
 597 varve isochrones. The latter are based on lateral correlation of basal varves and are drawn
 598 with 20 years interval. Indicated varve years for deglaciation is in the relation to the so called
 599 'zero year' in the Swedish varved clay chronology (Cato 1985, 1987). Measured youngest
 600 striae are marked from opposite sides of the esker/calving bays, indicating near-marginal ice
 601 flow re-adjustment (from the general ice flow direction north to south), being approximately
 602 perpendicular to the calving bay configuration at ice-margin gradual retreat. (A) The
 603 moderately indented calving bay gradually forming around the Uppsala esker at ice recession
 604 between varve years -1100 and -920 (180 years) over a distance of ~40 km (mean recession
 605 ~222 m/year). Note a slight increase with time in calving bay depth towards the north.
 606 Calving bay depths and widths are hard to define, but depths are only in the order of 2-4 km,

20

1
2
3 607 marked as shallow indentions in the close to west to east-trending receding ice margin. Centre
4 608 of the map is N59°43'; E17°36' (position marked with orange box in Fig. 1B). (B) The
5 609 strongly but variably indented calving bays gradually forming around the Enköping and Gävle
6 610 eskers at ice recession between varve years -800 and -700 (100 years) over a distance of ~47
7 611 km (mean recession ~470 m/year). Calving bay depths north of isochrone -800 vary between
8 612 6-15 km and widths between 6-17 km at bay mouths, with both calving bay depth decreases
9 613 and increases at gradual ice margin recession. Centre of the map is N60°25'; E16°53'
10 614 (position marked with orange box in Fig. 1B).

11
12
13
14 615 Fig. 3. Overview of Quaternary sediments and landforms in the Kumla–Örebro area. (A)
15 616 Extract of the Quaternary geology map Örebro SW (Fromm, 1972). For full legend, see online
16 617 version at <http://resource.sgu.se/produkter/ae/ae5-karta.pdf>. (B) Extract of De Geer moraines
17 618 (blue lines), eskers (green) and youngest striae (red bullet arrows) from (A). The north to
18 619 south trending Kumla esker has nearby De Geer moraines trending towards WSW to SW west
19 620 of the esker, while De Geer moraines east of the esker trend towards SE, indicating local ice
20 621 margin rearrangement from the general W–E trend around the esker and thus suggesting the
21 622 formation of a calving bay at the northwards retreat of the subaqueous ice margin (Bergdahl
22 623 1959, 1965; Fromm 1972). Place names Härminge, Brickebacken and Stora Ulvgryta, and
23 624 their black frames, indicate the positions of LiDAR-derived DEM scenes shown in Figs. 5, 7
24 625 and 8, revealing much denser patterns of De Geer moraines than shown here as based on
25 626 ground survey mapping.

26
27
28
29
30 627 Fig. 4. Overview LiDAR-based mapping of drumlins and De Geer moraines in the Kumla-
31 628 Örebro area (the same geographic extent as in Fig. 3). Drumlins are divided into large-scale
32 629 drumlins (black outlines) showing the same N-S trend as for the rest of the streamlined flow
33 630 sets of the Närke plain (Möller and Dowling, accepted), while the small-scale drumlins (red)
34 631 when occurring deviate from this regional direction, trending NW-SE and NE-SW on the
35 632 respective sides of the Kumla esker. De Geer moraines are perpendicular to the small-scale
36 633 drumlins and thus trend NE-SW and NW-SE on opposite sides of the said esker. Coverage of
37 634 the three zoomed in Lidar DEM's in Figs. 5, 7 and 8 are marked by black frames.

38
39
40
41 635 Fig. 5. LiDAR-based mapping of small-scale drumlins and De Geer moraines in the Härminge
42 636 subarea (geographic coverage shown in Fig. 4). Hillshade illumination is from 120° with an
43 637 azimuth of 25° and an x5 vertical exaggeration.

44
45
46 638 Fig. 6. A drone image (view towards NE) of De Geer moraines in the Härminge subarea
47 639 (Figs. 4 and 5). Five De Geer moraine ridges are here protruding through surrounding clay,
48 640 which are the agricultural fields in the fore- and mid-ground. The moraine closest to the
49 641 viewer is approximately 50 m long. The ridges trend NW-SE and tentative ice margins at their
50 642 formation are indicated by white hatched lines.

51
52
53 643 Fig. 7. LiDAR-based mapping of small-scale drumlins and De Geer moraines in the
54 644 Brickebacken subarea (geographic coverage shown in Fig. 4). Hillshade illumination is from
55 645 120° with an azimuth of 25° and an x5 vertical exaggeration. The colour ramp has been
56 646 inverted.

1
2
3 647 Fig. 8. LiDAR-based mapping of small-scale drumlins and De Geer moraines in the Stora
4 648 Ulvhytta subarea (geographic coverage shown in Fig. 4). Hillshade illumination is from 250°
5 649 with an azimuth of 25° and an x5 vertical exaggeration. The colour ramp has been inverted.
6

7
8 650 Fig. 9. Idealised ice flow re-organisation and calving bay formation (left-hand scenes). The
9 651 selected area is a random snapshot of the main Kumla esker body (pannels A, C and E), along
10 652 with an idealised geomorphological evolution sketch map (pannels B, D and F). The area in
11 653 front of the depicted calving embayments was occupied by the marine Yoldia Sea with water
12 654 depths in the order of 80-130 m. (A) Flow lines further back from the ice margin at formation
13 655 of the large-scale streamlined bed forms. (B) Large drumlinoids (black ellipses) developed
14 656 parallel to the regional ice flow direction further back from the receding ice margin. (C-D) A
15 657 calving bay is formed at ice margin recession (arbitrarily chosen time-transgressive position),
16 658 in which apex the esker (green line) formed as lined-up subaqueous fans at the subglacial
17 659 tunnel mouth. Ice flow (indicated by blue flow lines) was re-arranged from regional flow to
18 660 be adjusted perpendicular to the new ice margin configuration of the approaching calving bay.
19 661 De Geer moraines (blue lines) formed gradually at the receding ice margin at an ~30-35°
20 662 angle to the N-S directed esker. Small-scale drumlins (red) formed parallel to the near-
21 663 marginal flow lines. (E-F) The final stages of the calving bay, the bay has opened out and ice
22 664 flow is readjusting to a north-south direction. No small drumlins are seen to form with this
23 665 flow orientation. The De Geer moraines formed at this stage are not perpendicular to the small
24 666 drumlins formed early on.
25
26
27
28
29

30 667
31
32
33
34
35
36
37
38
39
40
41
42
43
44
45
46
47
48
49
50
51
52
53
54
55
56
57
58
59
60

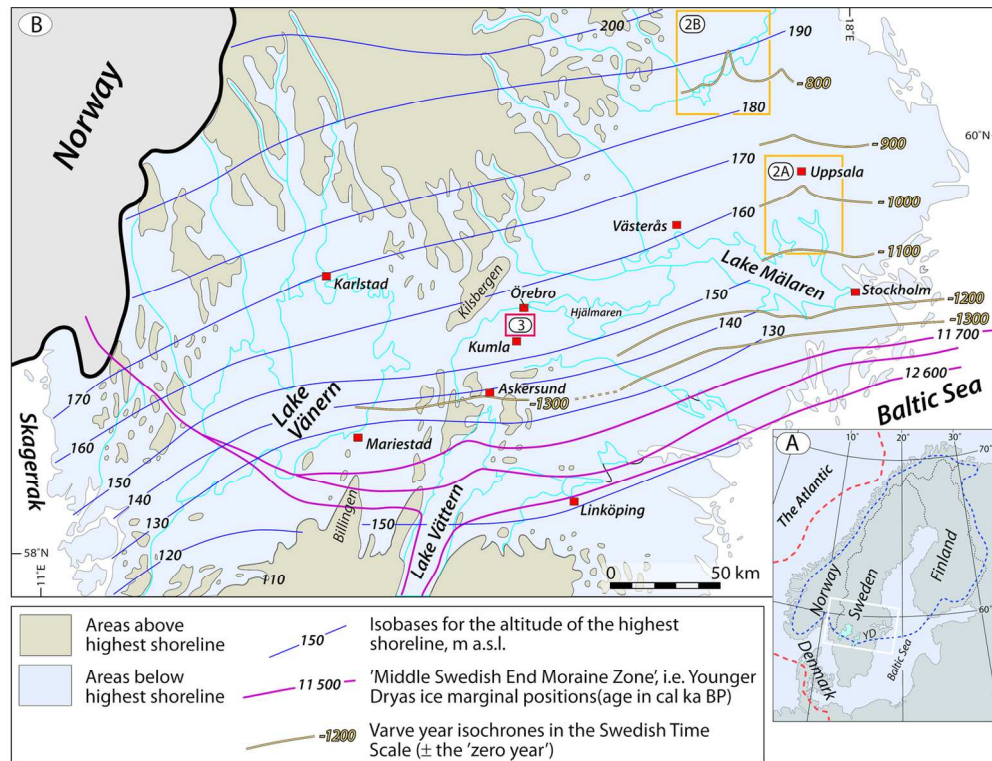


Fig. 1. (A) Overview of NW Europe. Red dashed line = proposed Fennoscandian Ice Sheet margin to the west/south at LGM (Svendsen et al., 2004); blue dashed line = the Younger Dryas Ice Marginal Zone (Mangerud et al., 2011). (B) Map of southern Sweden (for location, white box in (A)), showing areas above and below the highest shoreline (marine limit in the west), and altitude of the highest shoreline at deglaciation. The highest shoreline east of Billingen is the shore altitude for the Baltic Ice Lake prior to its 2nd drainage at retreat from Billingen after the Younger Dryas advance, while highest shoreline isobases north thereof were formed in the following Baltic Basin stages Yoldia Sea and Ancylus Lake (Björck, 1995), following the northwards receding ice margin. Inferred ice-marginal positions during the Younger Dryas are according to Lundqvist (2009). Deglacial varve isochrones are transferred from Brunnberg (1995) (south of Stockholm), Strömberg (1994) (Lake Vänern-Askersund) and Strömberg (1989) (north of Stockholm). Base map compiled from the Swedish National Atlas (Fredén, 2009). Red box marks the investigated area between Örebro and Kumla (Fig. 3) and orange boxes mark the positions of Figs. 2A and 2B. Typical ice flow for the local area was north-south.

137x104mm (300 x 300 DPI)

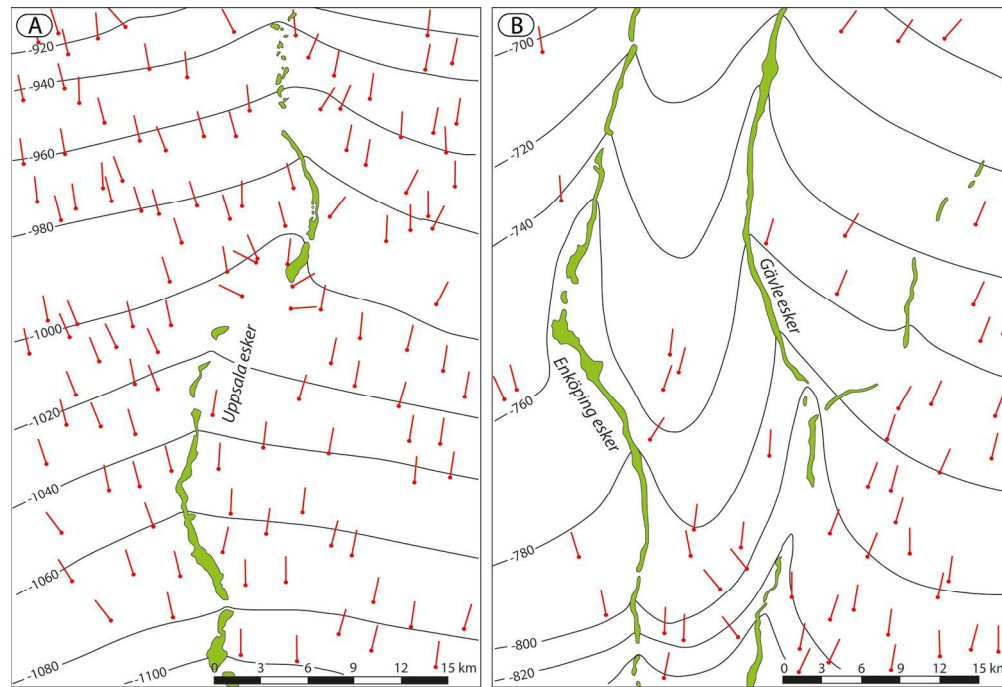


Fig. 2. Examples of reconstructed calving bays around some of the larger eskers north of Lake Mälaren, south-central Sweden (Fig. 1B), based on varved clay measurements (redrawn from Plates 2 and 3 in Strömberg (1989)). Eskers are shown in green, striae outcrop locations are marked with a red with the direction indicated by the red line and the black lines indicate varve isochrones. The latter are based on lateral correlation of basal varves and are drawn with 20 years interval. Indicated varve years for deglaciation is in the relation to the so called 'zero year' in the Swedish varved clay chronology (Cato 1985, 1987). Measured youngest striae are marked from opposite sides of the esker/calving bays, indicating near-marginal ice flow re-adjustment (from the general ice flow direction north to south), being approximately perpendicular to the calving bay configuration at ice-margin gradual retreat. (A) The moderately indented calving bay gradually forming around the Uppsala esker at ice recession between varve years -1100 and -920 (180 years) over a distance of ~ 40 km (mean recession ~ 222 m/year). Note a slight increase with time in calving bay depth towards the north. Calving bay depths and widths are hard to define, but depths are only in the order of 2-4 km, marked as shallow indentions in the close to west to east-trending receding ice margin. Centre of the map is $N59^{\circ}43'$; $E17^{\circ}36'$ (position marked with orange box in Fig. 1B). (B) The strongly but variably indented calving bays gradually forming around the Enköping and Gävle eskers at ice recession between varve years -800 and -700 (100 years) over a distance of ~ 47 km (mean recession ~ 470 m/year). Calving bay depths north of isochrone -800 vary between 6-15 km and widths between 6-17 km at bay mouths, with both calving bay depth decreases and increases at gradual ice margin recession. Centre of the map is $N60^{\circ}25'$; $E16^{\circ}53'$ (position marked with orange box in Fig. 1B).

721x491mm (72 x 72 DPI)

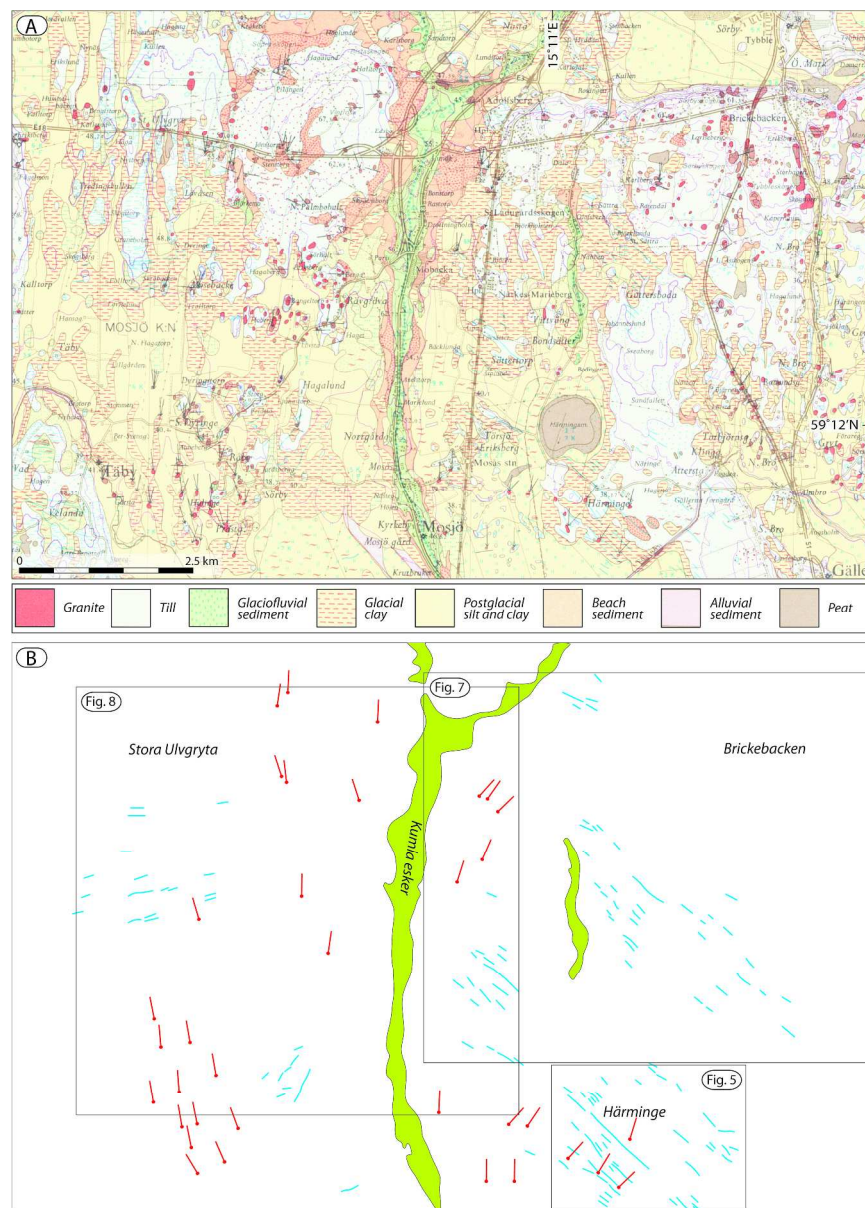


Fig. 3. Overview of Quaternary sediments and landforms in the Kumla-Örebro area. (A) Extract of the Quaternary geology map Örebro SW (Fromm, 1972). For full legend, see online version at <http://resource.sgu.se/produkter/ae/ae5-karta.pdf>. (B) Extract of De Geer moraines (blue lines), eskers (green) and youngest striae (red bullet arrows) from (A). The north to south trending Kumla esker has nearby De Geer moraines trending towards WSW to SW west of the esker, while De Geer moraines east of the esker trend towards SE, indicating local ice margin rearrangement from the general W-E trend around the esker and thus suggesting the formation of a calving bay at the northwards retreat of the subaqueous ice margin (Bergdahl 1959, 1965; Fromm 1972). Place names Härminge, Brickebacken and Stora Ulvgryta, and their black frames, indicate the positions of LiDAR-derived DEM scenes shown in Figs. 5, 7 and 8, revealing much denser patterns of De Geer moraines than shown here as based on ground survey mapping.

243x339mm (300 x 300 DPI)

1
2
3
4
5
6
7
8
9
10
11
12
13
14
15
16
17
18
19
20
21
22
23
24
25
26
27
28
29
30
31
32
33
34
35
36
37
38
39
40
41
42
43
44
45
46
47
48
49
50
51
52
53
54
55
56
57
58
59
60

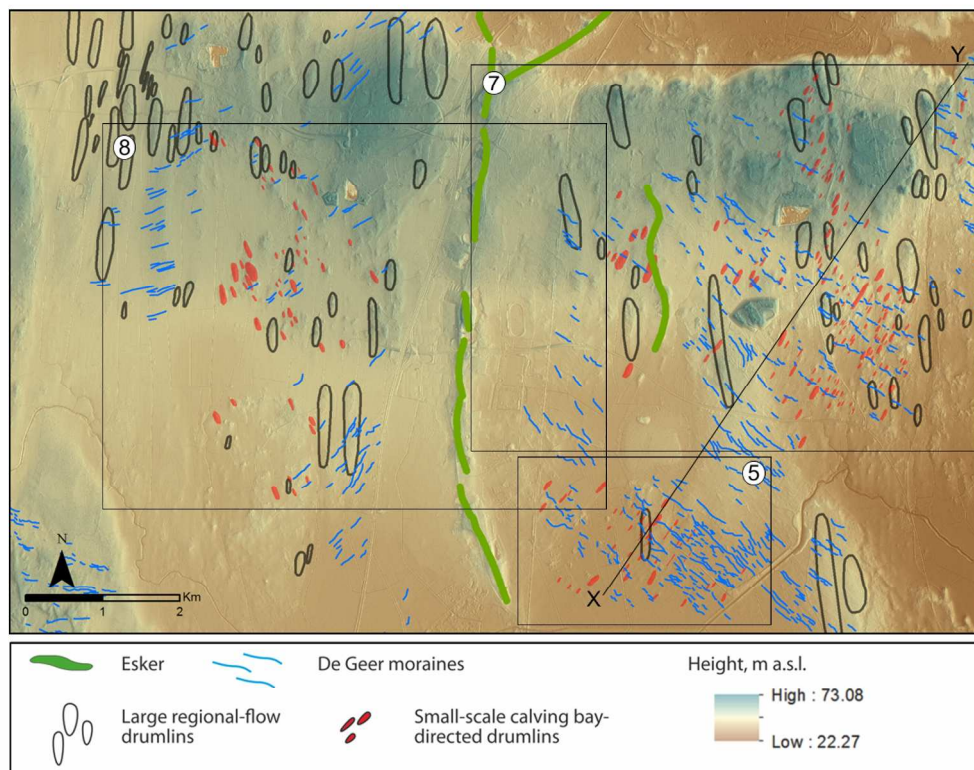


Fig. 4. Overview LiDAR-based mapping of drumlins and De Geer moraines in the Kumla-Örebro area (the same geographic extent as in Fig. 3). Drumlins are divided into large-scale drumlins (black outlines) showing the same N-S trend as for the rest of the streamlined flow sets of the Närke plain (Möller and Dowling, accepted), while the small-scale drumlins (red) when occurring deviate from this regional direction, trending NW-SE and NE-SW on the respective sides of the Kumla esker. De Geer moraines are perpendicular to the small-scale drumlins and thus trend NE-SW and NW-SE on opposite sides of the said esker. Coverage of the three zoomed in Lidar DEM's in Figs. 5, 7 and 8 are marked by black frames.

203x163mm (300 x 300 DPI)

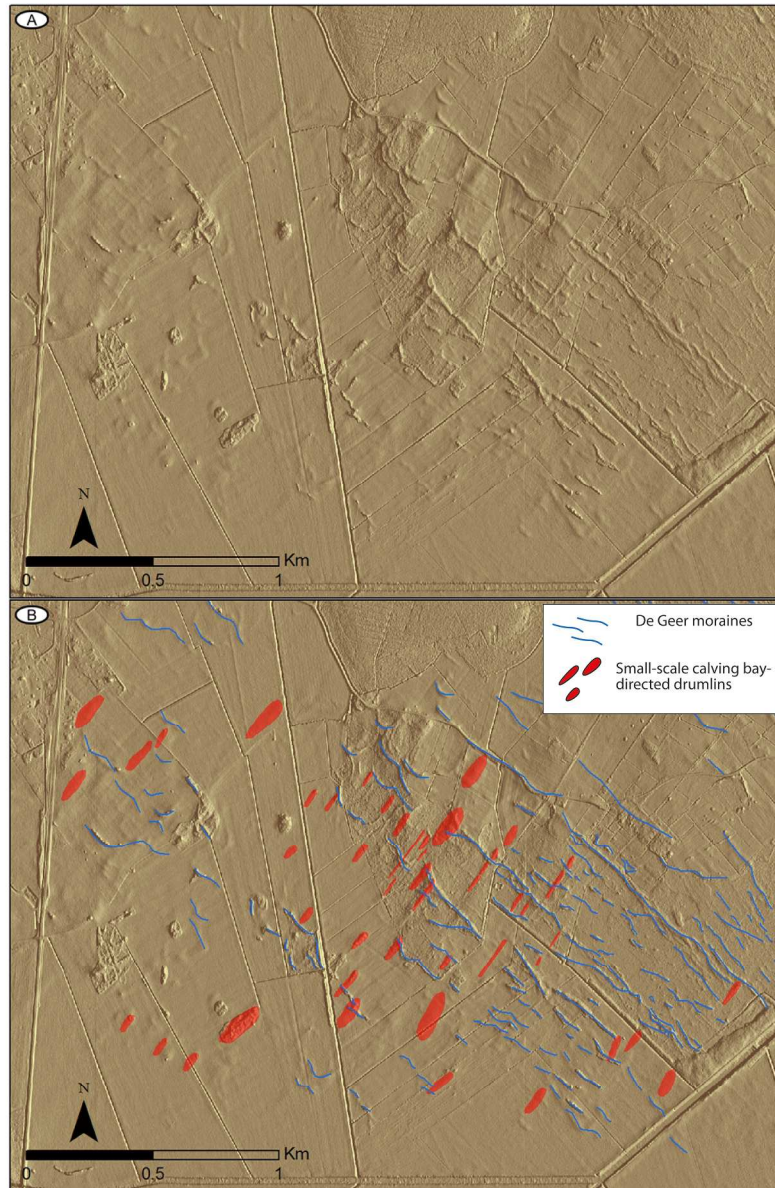


Fig. 5. LiDAR-based mapping of small-scale drumlins and De Geer moraines in the Härminge subarea (geographic coverage shown in Fig. 4). Hillshade illumination is from 120° with an azimuth of 25° and an x5 vertical exaggeration.

790x1116mm (72 x 72 DPI)

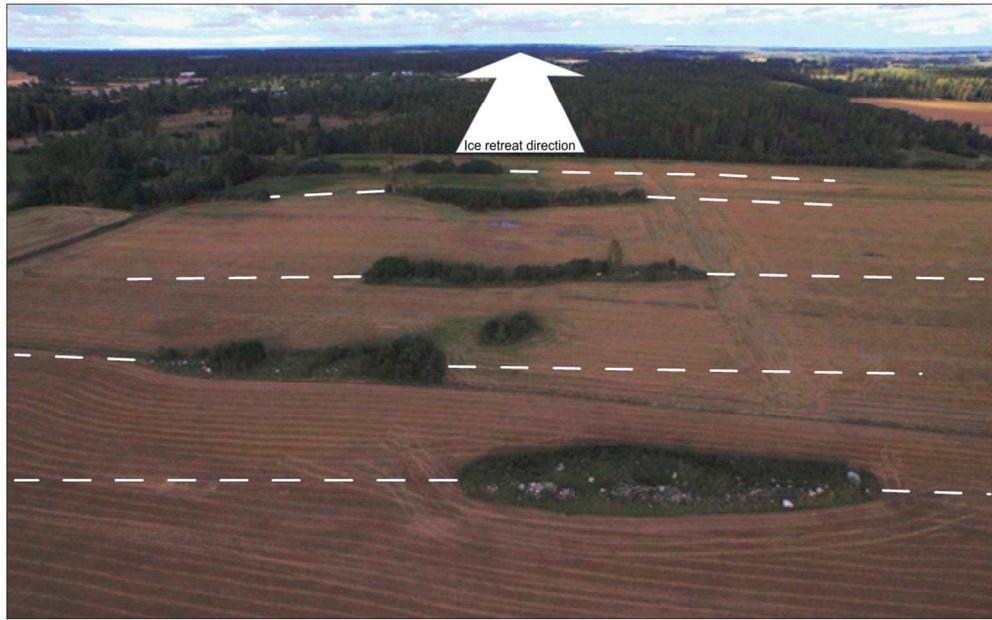


Fig. 6. A drone image (view towards NE) of De Geer moraines in the Härminge subarea (Figs. 4 and 5). Five De Geer moraine ridges are here protruding through surrounding clay, which are the agricultural fields in the fore- and mid-ground. The moraine closest to the viewer is approximately 50 m long. The ridges trend NW-SE and tentative ice margins at their formation are indicated by white hatched lines.

327x204mm (96 x 96 DPI)

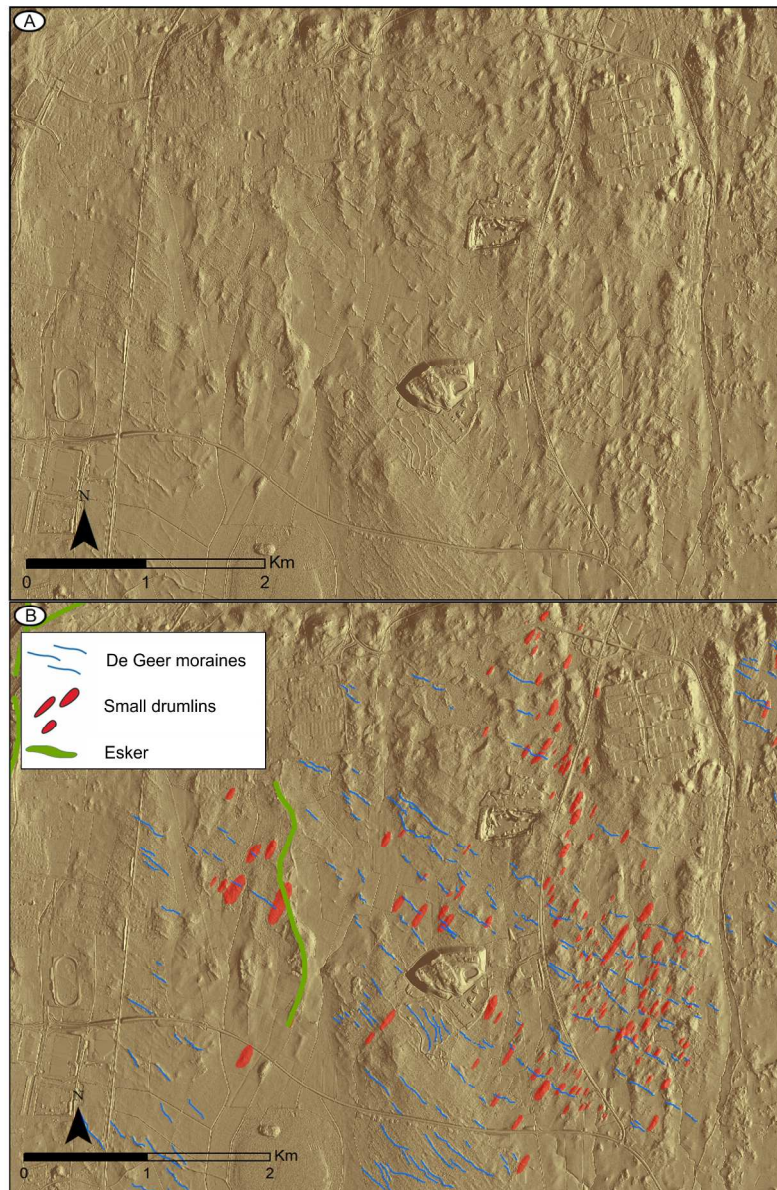


Fig. 7. LiDAR-based mapping of small-scale drumlins and De Geer moraines in the Brickebacken subarea (geographic coverage shown in Fig. 4). Hillshade illumination is from 120° with an azimuth of 25° and an x5 vertical exaggeration. The colour ramp has been inverted.

210x297mm (300 x 300 DPI)

1
2
3
4
5
6
7
8
9
10
11
12
13
14
15
16
17
18
19
20
21
22
23
24
25
26
27
28
29
30
31
32
33
34
35
36
37
38
39
40
41
42
43
44
45
46
47
48
49
50
51
52
53
54
55
56
57
58
59
60

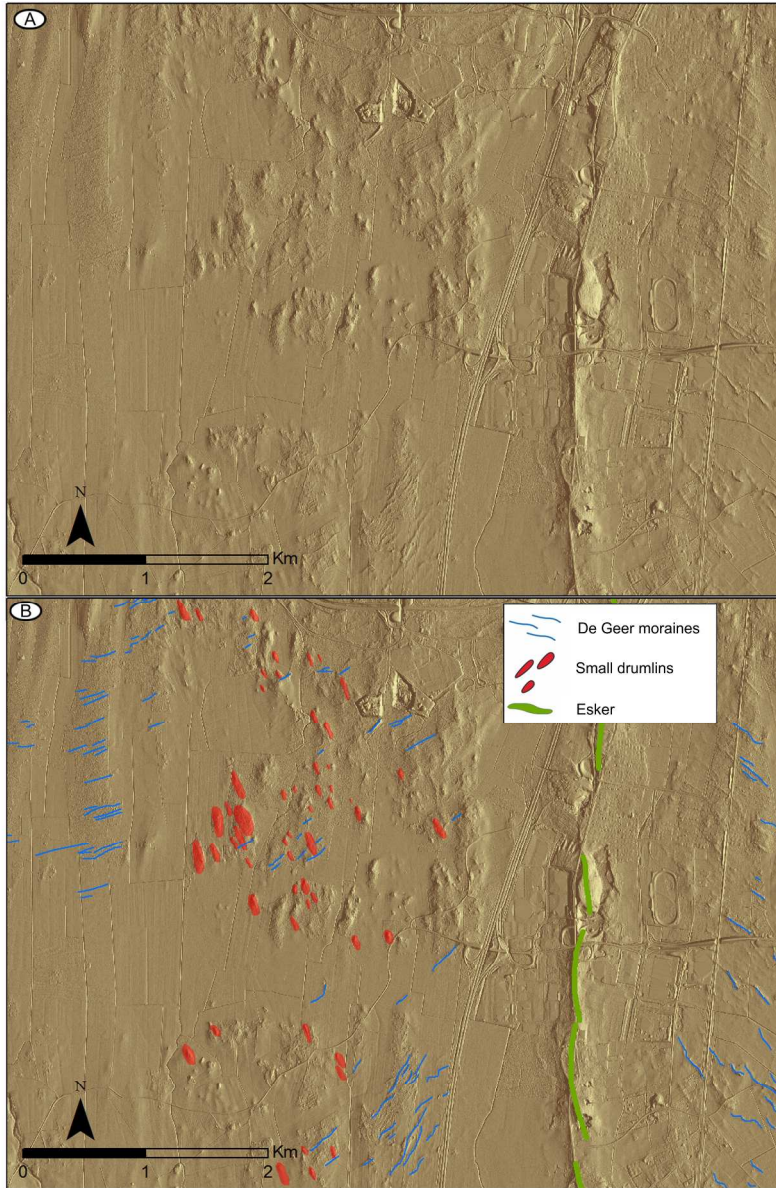


Fig. 8. LiDAR-based mapping of small-scale drumlins and De Geer moraines in the Stora Ulvhytta subarea (geographic coverage shown in Fig. 4). Hillshade illumination is from 250° with an azimuth of 25° and an x5 vertical exaggeration. The colour ramp has been inverted.

210x297mm (300 x 300 DPI)

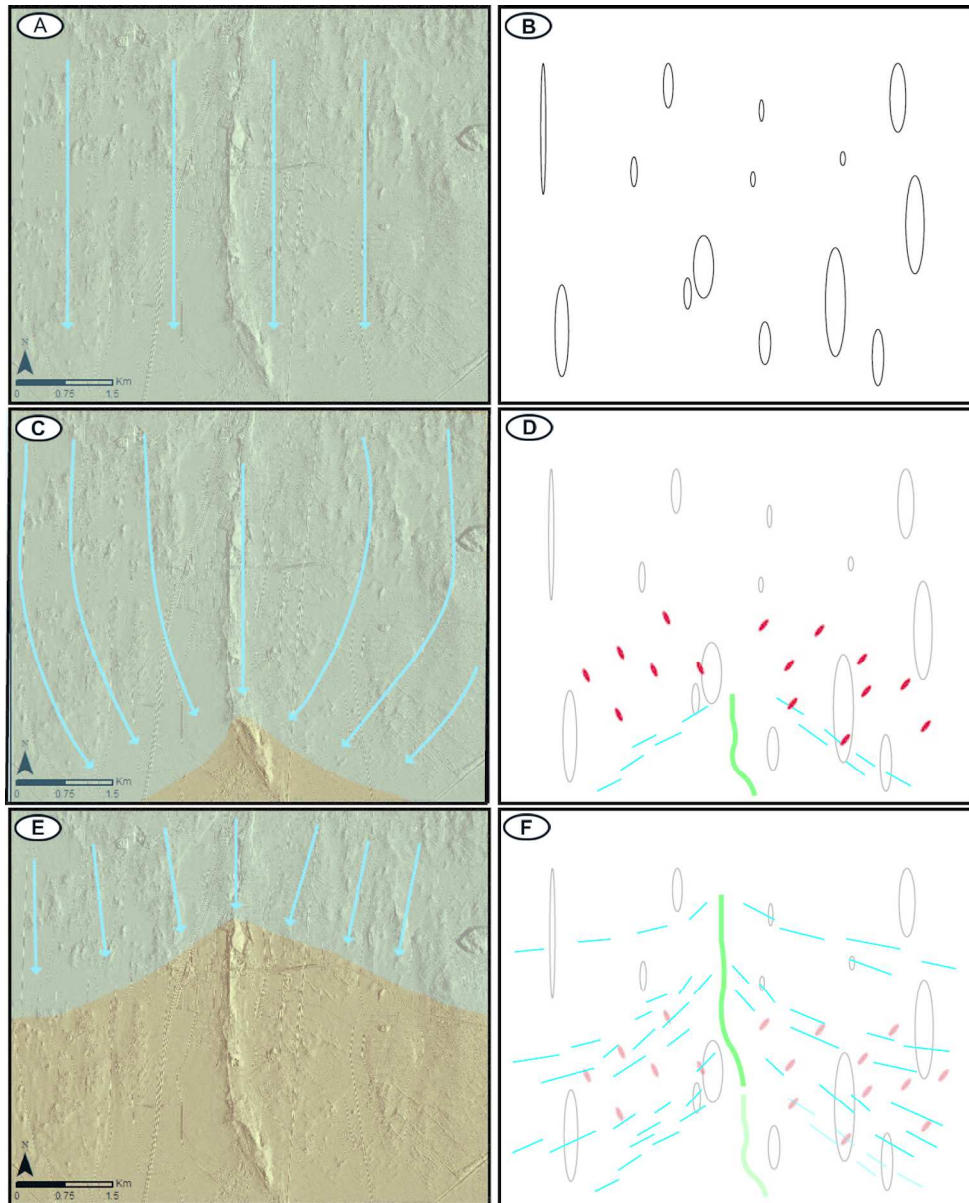


Fig. 9. Idealised ice flow re-organisation and calving bay formation (left-hand scenes). The selected area is a random snapshot of the main Kumla esker body (panels A, C and E), along with an idealised geomorphological evolution sketch map (panels B, D and F). The area in front of the depicted calving embayments was occupied by the marine Yoldia Sea with water depths in the order of 80-130 m. (A) Flow lines further back from the ice margin at formation of the large-scale streamlined bed forms. (B) Large drumlinoids (black ellipses) developed parallel to the regional ice flow direction further back from the receding ice margin. (C-D) A calving bay is formed at ice margin recession (arbitrarily chosen time-transgressive position), in which apex the esker (green line) formed as lined-up subaqueous fans at the subglacial tunnel mouth. Ice flow (indicated by blue flow lines) was re-arranged from regional flow to be adjusted perpendicular to the new ice margin configuration of the approaching calving bay. De Geer moraines (blue lines) formed gradually at the receding ice margin at an $\sim 30\text{-}35^\circ$ angle to the N-S directed esker. Small-scale drumlins (red) formed parallel to the near-marginal flow lines. (E-F) The final stages of the calving bay, the bay has opened out and ice flow is readjusting to a north-south direction. No small drumlins

1
2
3
4
5
6
7
8
9
10
11
12
13
14
15
16
17
18
19
20
21
22
23
24
25
26
27
28
29
30
31
32
33
34
35
36
37
38
39
40
41
42
43
44
45
46
47
48
49
50
51
52
53
54
55
56
57
58
59
60

are seen to form with this flow orientation. The De Geer moraines formed at this stage are not perpendicular to the small drumlins formed early on.

418x515mm (300 x 300 DPI)

1
2
3
4
5
6
7 **1 Rapid subglacial streamlined bedform formation at a calving bay**
8 **margin**
9

10 3 THOMAS P.F. DOWLING^a, PER MÖLLER^a and MATTEO SPAGNOLO^b
11
12 4

13
14 5 ^aDepartment of Geology, Quaternary Sciences, Lund University, Sölvegatan 12, SE 22362
15
16 6 Lund, Sweden. ^bGeography & Environment Department, School of Geosciences, University
17
18 7 of Aberdeen, Aberdeen AB24 3UF, UK
19

20 8 **ABSTRACT:** Using the LiDAR derived Swedish national height model we have identified
21
22 9 previously undescribed shallow streamlined glacial bedforms, small-scale drumlins, on the
23
24 10 Närke plain in south-central Sweden. These drumlins could only be detected with high
25
26 11 resolution LiDAR, due to both their subtle size and forest cover. In this area the ice margin
27
28 12 receded in a subaqueous environment with a proglacial water depth in the order of 100 m
29
30 13 during the last deglaciation. As indicated by the configuration of marginally formed De Geer
31
32 14 moraine ridges draping the drumlinoids, the receding ice margin formed deeply indented
33
34 15 calving bays. These were located around subaqueous outlets of the subglacial melt-water
35
36 16 drainage, with their apex position marked geomorphologically by beaded esker ridges. The
37
38 17 mapped small-scale drumlins are aligned perpendicular to the reconstructed ice sheet margin
39
40 18 and suggest formation along flow lines adjusted to the configuration of these calving
41
42 19 embayments as they propagated up-flow with ice margin retreat. Based on these geometric
43
44 20 relationships we argue that the emplacement of the drumlins was near-marginal, ~7.7-1 km
45
46 21 from the margin, on a short timescale (~5-35 years).
47

48 22 **Running title:** Flow reorganisation at calving bay margin quickly constructs drumlins.
49

50
51 23 **KEYWORDS:** streamlined terrain, drumlin, calving bay, De Geer moraine, ice recessional
52 24 history

53 25 Correspondence to T. P. F. Dowling, as above

54 26 E-mail: tom.dowling@geol.lu.se
55
56
57
58
59
60

27 Introduction

28 Streamlined subglacial bedforms, such as drumlins, are common geomorphic features on the
29 relict ice beds of formerly glaciated regions. ~~As such, they and~~ have drawn intense research
30 attention as their formation is considered key for understanding ice sheet dynamics. Many
31 theories, widely inspired by various morphometric and sedimentological observations, have
32 been put forward regarding the formation of drumlins, but the debate is far from closed (see
33 discussions in, e.g., Clark, 2010; Stokes et al., 2011; Eyles et al., 2016; Möller and Dowling,
34 2016). Two aspects of key relevance that have perhaps seen relatively less attention,
35 especially in recent years, are *where* drumlins form with respect to the ice margin and the *time*
36 *frame* in which they form.

37 From a process point of view the location of formation for a drumlin must meet some
38 combination of sediment erosion, transport and/or deposition. These three elements are in turn
39 dependent on a number of things, including basal ice flow velocity and the induced basal
40 shear stress on the subglacial sediment. The latter is highly dependent on the effective stress
41 (normal stress reduced by pore water pressure) induced by the glacier at its bed. All of these
42 parameters will vary along any given flow line and the resulting criteria for drumlin formation
43 may be met sporadically or continuously throughout time. There are thus likely to be zones
44 where basic conditions for bedform formation are met better than in other places due to
45 presence of obstacles and/or a significant sediment supply (Stokes et al., 2013).

46 Drumlins are often described as forming within the main body of ice sheets (Raukas and
47 Tavast, 1994), generally in areas of fast flow (ice streams) and at significant distances from
48 the margin (Wellner et al., 2001). However, other studies suggest that they may also form
49 relatively close to ice margins (Menzies, 1979). For example, Glückert (1973, 1987) describes
50 drumlin fields in the central lake district of Finland that form outwards diverging flowsets
51 along flow lines adjusted to the lobate configuration of the Younger Dryas ice-marginal zone,
52 less than 100 km from that ice margin and over a single short ice streaming event. Other
53 examples of near-marginal streamlining include the SE Baltic where Lamsters and Zelčs
54 (2014) show that drumlins ~~formformed~~ flow sets that diverge towards strongly lobate ice-
55 marginal positions, as marked by end moraine zones. More recently at Múlajökull, Iceland,
56 Johnson et al. (2010) have suggested that drumlins might form at the very margin of a surging
57 glacier.

1
2
3
4
5
6
7 58 There is relatively little in the literature that considers the chronological aspect of drumlin
8 59 formation as there is both a dearth of syn-formational observations and a lack of dateable
9 60 material within the features themselves. However, the time period in which a feature forms is
10 61 a critical component in efforts to reconstruct past ice sheets from the relict landscape. Of the
11 62 evidence thus far gathered there is a wide disparity in suggestions of how fast or over which
12 63 time frames subglacial bedforms are formed; Hättestrand et al. (2004) have suggested that
13 64 large drumlins in northern and central Sweden are the result of sediment accretion from
14 65 multiple glaciations and therefore have a very long formation time. In contrast to this, Smith
15 66 et al. (2007) and King et al. (2009) found that the formation of contemporary subglacial
16 67 features under an Antarctic ice stream are formed and evolve on the time scale of a few years.
17 68 Rapid formation times are also suggested from the work of Johnson et al. (2010).

18
19
20
21
22
23 69 In this paper we investigate the time of formation of a number of small drumlins mapped
24 70 within the streamlined terrain on the Närke plain, an area situated in south-central Sweden
25 71 (Fig. 1), using high-resolution LiDAR-derived topographic data. The spatial association of
26 72 these smaller features with nearby esker and De Geer moraine complexes is here investigated.
27 73 In particular, the geometry of these landforms, their relationships with both one another and
28 74 to the Swedish varve chronology, all provide an indication of where the small-scale drumlins
29 75 formed in relations to the retreating margin of the Fennoscandian Ice Sheet and the amount of
30 76 time it took them to form.

31 77 **Regional and local geologic setting of the study area**

32
33
34
35
36
37
38 78 The Närke plain in the Kumla–Örebro area, south-central Sweden (Fig. 1), on which the
39 79 drumlins investigated here are located, is a low-elevation area at ~30-80 m above present-day
40 80 sea level (m a.s.l.). Below the covering Quaternary deposits are down-faulted and tilted blocks
41 81 of crystalline basement, overlain in varying occurrence by Palaeozoic sandstone, clay slate,
42 82 alum shale and limestone, in that stratigraphic order (Ericsson, 1979).

43
44
45
46 83 During the deglaciation of the Kumla–Örebro area (Fig. 1), the subsequent northwards ice
47 84 recession was primarily subaqueous with the retreating ice margin standing in water depths
48 85 often in excess of 100 m (sea level at deglaciation, c. 150-160 m a.s.l. (Fig. 1), minus present-
49 86 day elevation). The area was deglaciated in conjunction with a marine ingression from the
50 87 west into the Baltic Basin (Brunnberg, 1995) a few hundred years after the final drainage of
51 88 the Baltic Ice Lake at Mount Billingen (11.62 cal ka BP according to Stroeven et al. (2015)).

1
2
3
4
5
6
7 89 | ~~in press~~). Thus, at deglaciation the water basin in front of the receding ice margin changed
8 90 from freshwater conditions to marine with the onset of the Yoldia Sea (Brunnberg, 1995; J.
9 91 Björck et al., 2001). This saline environment is indicated by the occurrence of the marine mollusc
10 92 *Portlandia (Yoldia) arctica* in the lowermost clay of the area (Bergdahl, 1961). Also due to the
11 93 marine environment at deglaciation, suspended clay was prone to flocculation (Krank, 1973;
12 94 Skei and Syvitski, 2013) resulting in poorly developed (symmict) varves or close to massive
13 95 clay, thus making a complete annual varve reconstruction, based on clastic rather than
14 96 symmict varves, not possible for this area. Indeed, Nilsson (1968) reports a maximum of only
15 97 48 annual varves from the area within the basal section of the up to 5-10 m thick fine-grained
16 98 subaqueous deposits, which was not enough to construct a detailed varve chronology.

17
18
19
20
21
22 99 Varved clay chronology is based on the between-site lateral correlation of peaks in vertically
23 100 measured and graphically plotted summer/winter bed thicknesses for specific sites; the
24 101 'classical' method as described in De Geer (1940) is to count the difference in basal 'missing'
25 102 varves between two sites which then is a measure of difference in deglaciation age in years
26 103 between the two sites. From these differences in deglacial age, varve isochrones are
27 104 | interpolated; in the case of the varve chronology from the Stockholm-Uppsala [area](#) (Fig. 2)
28 105 this was done in 20 year steps. The basal varves formed close to the receding ice margin and
29 106 the constructed varve isochrones thus mirror not only deglaciation time but also the
30 107 configuration of the ice margin in temporal steps during continuous ice margin recession.

31
32
33
34
35
36 108 In addition to the Stockholm-Uppsala chronology northeast of our study site a detailed and
37 109 precise varved clay chronology has been reconstructed just south of our investigated area,
38 110 between Västergötland (Strömberg, 1994) and Närke/Östergötland (Brunnberg, 1995; J.
39 111 Björck et al., 2001). This chronology can be extended to provide an overall indication of the
40 112 deglaciation time just south of the Kumla–Örebro region. The -1200 varve isochrone of
41 113 Brunnberg (1995) trends directly south of Kumla (Fig. 1) and the deglaciation of the Kumla–
42 114 | Örebro [area](#) should thus have occurred between the -1200 and -1100 isochrones. As the 'zero
43 115 year' (± 0) in the Swedish time scale is set to 10 090 cal yr BP (Stroeven et al., 2015), this is
44 116 | equivalent to c. 11.3 – 11.2 cal ka BP (Stroeven et al., ~~2015~~~~in press~~) as an approximate
45 117 deglaciation age for the Kumla–Örebro area.

46
47
48
49
50
51 118 Eskers in the area have a general S-N trend on the Närke plain (Fromm, 1972; Ericsson,
52 119 1979). This concurs with the general glacial striae pattern, varying between N10°W and N10

1
2
3
4
5
6
7 120 'E, and the primary drumlin flow sets, indicating the regional ice flow direction (Möller and
8 121 Dowling, 2016). The eskers occur with 4 to 9 km wide gaps between them, as calculated from
9 122 7 eskers identified from the Quaternary deposits maps of the area (Fromm, 1972; Ericsson,
10 123 1979) over a 40 km long profile from west to east. Central through the Kumla-Örebro area
11 124 runs the Hallsberg-Kumla esker; although this is the 'official' name (Bergdahl, 1961), it will
12 125 in the following be called the 'Kumla esker' for short. Parts of these eskers formed infra-
13 126 marginally as subglacial tunnel fillings, but most of the glaciofluvial sediment was deposited
14 127 as tunnel mouth subaqueous fans of varying widths lined up after each other as the ice margin
15 128 retreated (De Geer, 1897). Such types of eskers, along with more modern facies models for
16 129 their formation, have been described as beaded eskers by Bannerjee and McDonald (1975) or
17 130 as subaqueous short bead fan eskers by Warren and Ashley (1994).

18 131 A frequently occurring feature at deglaciation in this part of Sweden was the formation of
19 132 large, often highly indented calving bays that during their existence were closely associated
20 133 with the larger eskers of south-central Sweden. The first description of these paleo-bays was
21 134 as early as Frödin (1916), who named them 'glaciofluvial estuaries' due to their connection to
22 135 eskers. The more general concept of calving bays at subaqueously retreating ice margins was
23 136 introduced by Hoppe (1948, 1957) for the Fennoscandian Ice Sheet. Calving bays formed
24 137 close to the larger eskers due to intensified – possibly intermittent – calving (see later
25 138 discussion), induced at, and lateral to, the mouth of subglacial drainage channels which also
26 139 were depocenters for the formation of De Geer eskers. The calving bays propagated
27 140 backwards, following the general retreat of the ice margin. The outlines of such calving bays
28 141 are often indicated from striae on bedrock outcrops close to the larger eskers and the
29 142 orientation of near-by De Geer moraines (Strömberg, 1981). The older regional-flow striae
30 143 from north to south are often then seen to be cut by younger striae coming from ~NE, east of
31 144 the eskers, and from ~NW, west of the eskers (e.g., as described in fig. 3 in Magnusson
32 145 (1984)). Examples of calving bays associated with eskers from the Stockholm-Uppsala
33 146 region, not far from the studied Kumla-Örebro area, are shown in Fig. 2 (reproduced from
34 147 Strömberg, 1989). Here, calving bays of varying depths into the receding ice margin are also
35 148 indicated from the configuration of reconstructed ice recession lines, in turn based on data
36 149 from varve measurements (varve isochrones) (e.g. Strömberg, 1981, 1989).

37 150 The strongest indicator for the existence of calving bays around eskers is, however, the
38 151 configuration of subaqueously formed ice-marginal moraines, generally known as De Geer
39 152 moraines (e.g. Lindén and Möller, 2005). These moraines occur in a bimodal distribution in

1
2
3
4
5
6
7 153 ~~Sweden, one population is located in the coastal area of north-eastern Sweden and the other~~
8 154 ~~as such moraines occur in~~ a broad belt across the deglacial subaqueous part of south-central
9
10 155 Sweden (Fredén, 2009; map on p. 134; [Bouvier et al., 2015](#)). ~~A significant pattern for this~~
11 156 ~~southern De Geer moraine belt is that that the ridges at~~. At a distance from the eskers ~~these~~
12 157 ~~ridges~~ are arranged approximately perpendicular to the esker trends, regional striae direction
13
14 158 and drumlins, ~~while closer~~ ~~Closer~~ to the esker ridges ~~they~~, ~~De Geer moraine ridges~~ usually
15 159 turn in orientation, coming in at an increasingly oblique angle to an esker on both sides. This
16
17 160 relationship is seen from the Quaternary deposits map of the Kumla–Örebro area (Fromm,
18 161 1972) (Fig. 3A) and is highlighted by the extraction of De Geer moraines and striae (Fig. 3B).
19
20 162 This pattern has also been described from studies of aerial photographs over the area in the
21 163 past (Bergdahl, 1959, 1961, 1965). Taken together, the geometric relationship between De
22 164 Geer moraines and the Kumla esker indicates that the studied area was also occupied by a
23
24 165 highly indented calving bay during ice retreat.

26 166 **Materials and methods**

27
28
29 167 The topographical data used in this paper is the LiDAR derived digital elevation model
30 168 (DEM) supplied by the Swedish national mapping agency (Lantmäteriet;
31 169 <http://www.lantmateriet.se>). This arrives to the end user with an average vertical accuracy of
32 170 ~0.1 m and a pixel resolution of 2 m. The data is pre-processed to remove both vegetation
33 171 cover and urban areas down to ‘true’ ground level. The technical details for this height model
34 172 can be found in Dowling et al. (2013). Data handling was carried out in ArcGIS[®] 10.0 and
35 173 Matlab[®] R2014^a.

36 174 Mapping of the landforms was manually carried out on hill-shade models illuminated from a
37 175 variety of angles. The small scale drumlins are only visible with x5 height exaggeration
38 176 applied and the careful manipulation of the angle of illumination. Typically the best angle of
39 177 illumination with which to see these features is either from 120° or 250°. Switching between
40 178 these angles and 90° reveals the small, shallow, drumlins. The mapping itself was carried out
41 179 as part of the work outlined in Dowling et al. (2015), and the drumlins are part of that larger
42 180 dataset. Height was extracted using the method of Spagnolo et al. (2012), whilst length and
43 181 width were extracted using minimum bounding geometry (Napieralski and Nalepa, 2010).

52 182 **Results**

183 *Landform descriptions*

184 The studied Kumla–Örebro area (~13 by 8 km), depicted in Figs. 3 and 4, contains
185 streamlined bedforms (drumlins) in two size ranges (Fig. 4). The larger features are typically
186 430-2200 m long, 110-400 m wide, and 8-15 m high (Table 1) and, when compared to the
187 metrics of global datasets (Clark et al., 2009; Spagnolo et al., 2012), could be considered
188 ‘classic’ drumlins. These drumlins are part of the general streamlined flow set of the wider
189 region of the Närke plain and are aligned approximately north to south (Möller and Dowling,
190 2016). The second size range of streamlined bedforms is an order of magnitude smaller and is
191 distributed at an angle to these larger features. Perpendicularly overlaid on these small-scale
192 drumlins are suites of De Geer moraines (Fig. 4). The distribution of, and relations between,
193 these geomorphic forms are further detailed in our LiDAR-derived DEMs over three chosen
194 smaller type areas, the Härminge and Brickebacken sub-areas, to the east of the Kumla esker
195 (Figs. 5 and 7), and the Stora Ulvgryta sub-area, to the west of said esker (Fig. 8).

196 The features in the Härminge sub-area (Fig. 5) clearly indicate the calving-bay orientation
197 relationship between small-scale drumlins, De Geer moraines and the esker. The area (~7
198 km²) hosts small-scale drumlins ($n = 48$) that ~~are vary-between~~ 41-245 m long and 10-71 m
199 wide, with a P_{10} - P_{90} height of 0.4-1.8 m (Table 1). Drumlin axes are orientated ~35/215°.
200 Draped over the drumlins is a dense set of De Geer moraines (Fig. 6), all trending ~305/125°.
201 These are thus perpendicular to the Härminge small-scale drumlins, but skewed relative to the
202 larger drumlins (e.g. right-hand side on Fig. 5). The De Geer moraines in the Härminge area
203 (Fig. 5) ~~measure-between~~ 25-832 m in length, 10-21 m in width and 2-3 m in height. The
204 Härminge small-scale drumlins and the De Geer moraines associated with them are thus at an
205 angle of ~38° to the north-south esker trend. It should be noted that for both the De Geer
206 moraines and especially for the small-scale drumlins in this sub-area there is the potential for
207 a shrouding effect (Finlayson, 2014; Spagnolo et al., 2014) when surrounded by on-lapping
208 glacial/postglacial aquatic sediments (silt and clay; Fig. 3). In some areas with deep
209 successions of aquatic sediments and/or organic deposits this shrouding effect can be several
210 meters (e.g., Möller and Dowling (2016) for the nearby Hackvad drumlin field); this can come
211 close to completely ‘drowning’ smaller geomorphic features.

212 The Brickebacken sub-area (Fig. 7) is due north of the Härminge sub-area (Fig. 4), covering
213 about 24 km². Small-scale drumlins in this set ($n = 155$) are 68-176 m long, 17-57 m wide and
214 1.5-2.3 m high (P_{10} - P_{90} values). Drumlin axes are orientated ~35/215°, i.e. the same direction

1
2
3
4
5
6
7 215 | as at Härminge, but these features are here more densely packed. Bedrock outcrops associated
8 216 | with the drumlins are often detectable from the Quaternary mapping and from visual
9 217 | inspection of the hill shade model, suggesting that mapped drumlins are of the rock-cored
10 218 | type. As at Härminge, the drumlins are superimposed by De Geer moraines that trend
11 219 | $\sim 305/125^\circ$, although some of the moraines start to shift towards a $\sim 290/105^\circ$ alignment
12 220 | towards the eastern margin of the demarcated area. The De Geer moraines are 12-264 m long,
13 221 | ~ 20 -21 m wide and ~ 1 -2 m high. The shrouding effect is likely minimal here, as the features
14 222 | are located on a slightly elevated till plain with no subaquatic sediments preserved between
15 223 | moraine ridges. However, just outside of our mapped subarea there are features drowned in
16 224 | subaquatic fine-grained sediment which are now only visible as crop marks in aerial photos
17 225 | and as faint shadows in the hillshade models.

18 226 | The Stora Ulvgryta -sub-area (Fig. 8) is situated west of the Brickebacken area, covering
19 227 | about 30 km². Importantly, it is located on the western side of the Kumla esker (Fig. 4). The
20 228 | small-scale drumlins in this set ($n = 54$) have the same general pattern of morphometrics as
21 229 | the sub-areas on the eastern side of the esker. The drumlins are 65-241 m long, 22-70 m wide
22 230 | and 1-3 m high (P_{10} - P_{90} values) and have axes orientated $\sim 350/170^\circ$. Rock outcrops
23 231 | associated with the mapped drumlins are often detectable from the Quaternary mapping and
24 232 | the hill shade model. The drumlins are sparsely distributed and overlain by a small number of
25 233 | De Geer moraines that are 55-183 m long, ~ 14 -21 m wide and ~ 0.5 -1 m high, trending
26 234 | $\sim 70/250^\circ$.

27 235 | Taken together, the orientation of the small drumlins and their associated De Geer moraines
28 236 | on opposite sides of the Kumla esker provide strong evidence of the geometric development
29 237 | of the calving bay and ice margin retreat in the Kumla-Örebro region, as well as indicating the
30 238 | local, late-stage ice flow direction.

31 239 | **Discussion**

32 240 | *Advantages of using LiDAR terrain data*

33 241 | Without high resolution LiDAR it would be impossible to detect the small-scale drumlin
34 242 | features described here. Their small size, in particular their shallow height, makes their
35 243 | detection in the field or from traditional aerial photograph mapping very difficult. This is
36 244 | especially the case when located under forest cover, making the capability of LiDAR to 'look
37 245 | through' vegetation as important as a high spatial resolution for their detection. The work

1
2
3
4
5
6
7 246 done here shows the ability of high resolution LiDAR datasets to create detailed
8 247 reconstructions of palaeo-landform assemblages, combining both previously identified
9 248 landforms and newly identified relationships between these landforms with newly discovered
10 249 features. Furthermore, the mapping of De Geer moraines with LiDAR-based DEM's results in
11 250 much denser and detailed patterns as compared to previous ground- and aerial photograph-
12 251 based mapping ([see also Bouvier et al., 2015](#)); This enhancement is very evident when
13 252 comparing their mapped distributions in Fig. 3B versus Figs. 4, 5, 7 and 8. This further
14 253 strengthens any assessment of probable calving bay configuration.

18 254 *Palaeo-calving bay formation*

20 255 The pattern and direction of near-to-esker De Geer moraines provide evidence that the
21 256 receding ice margin formed pronounced indentions – a calving bay – around the Kumla esker
22 257 that formed transgressively backwards at the subaqueous outlet of the subglacial drainage at
23 258 deglaciation of the area. As the bay retreated northwards it also opened out, i.e. the angle
24 259 between the ice-front and the esker/drainage outlet increased as the margin moved north (see
25 260 Fig. 9 and mapping in Fig. 4).

26 261 The retreat of water-terminating ice margins is due to a balance of and feedbacks between
27 262 calving, topography and atmospheric warming (e.g. Venteris, 1999; Cook et al., 2005; Benn et
28 263 al., 2007a). Localized areas with higher ice loss over longer or shorter time periods, caused by
29 264 preferential calving at an active sub-surface drainage outlet (Benn et al., 2007b), might thus
30 265 result in concave calving bays. According to Benn and Evans (2010) this is most likely the
31 266 result of longitudinal extension occurring in conjunction with simple shear at the ice margin.
32 267 The effect of this is to generate distinctive crevasse patterns along which the enhanced calving
33 268 occurs, forming the concave planform of calving bays near eskers. An important factor in a
34 269 given calving rate is water depth (Benn et al., 2007a); postulated palaeo calving bays across
35 270 the subaqueously deglaciated south-central part of Sweden (Fig. 1) were evidently tied to the
36 271 positions of the larger eskers of this area. This might indicate the importance of this factor: the
37 272 eskers are usually situated in the lowermost positions of this once submerged landscape.

38 273 However, water depth differences along the receding ice margin were not that large. Possibly
39 274 more important in controlling calving rate was the *per se* existence of the subglacial drainage
40 275 conduits, marked in their deglacial positions by the resulting eskers. Melting of the ice above
41 276 these conduits and in their immediate surroundings would thin the ice, reduce basal effective
42 277 stresses and thus basal drag, introduce positive feedback into dynamic thinning and

1
2
3
4
5
6
7 278 propagation of deep surficial crevasses up-glacier, thus resulting in localized increases in
8 279 calving rate (e.g. Benn et al., 2007; Benn and Evans, 2010). A continuous fast differential ice
9 280 loss close to the eskers as compared to the areas between the eskers would, however,
10 281 theoretically mean that the calving bays would get progressively deeper with time.

12
13 282 When scrutinizing the maps of calving bay configurations as suggested from constructed varve
14 283 isochrones, e.g. Strömberg (1989), see Fig. 2B, or further north in the county of Dalarna
15 284 (Fromm, 1991) with very deep calving bays, it is evident that there was a tendency for calving
16 285 bays to grow progressively deeper with time, but only over portions of their recessional paths.
17 286 This suggests that the calving rate in the calving bays was larger than the regional ice recession
18 287 rate only over shorter periods of time, i.e. intermittent periods of fast calving. This was
19 288 followed by a reduction in the rate of ice loss back to the typical regional ice recession rate
20 289 with the generated calving bay configuration moving back into a more typical marginal
21 290 alignment.

22 291 *Location of drumlin formation and ice flow adjustment*

23
24
25
26
27 292 Based on their perpendicular relationship with the ice-marginal De Geer moraine ridges we
28 293 argue that the orientation of the small-scale drumlins in the Kumla-Örebro area, as depicted
29 294 in Fig. 4, reflects the direction of ice flow near the Kumla esker at a late stage of deglaciation.
30 295 The smaller-scale drumlins formed within a near-marginal area where the regional north to
31 296 south-directed ice flow had shifted as a response to the formation of an indented calving bay
32 297 (Fig. 9). The orientation of De Geer moraine ridges changes slightly throughout the study area
33 298 as the ice margin geometry was modified during retreat. However, these differences are too
34 299 small to be able to associate individual drumlins to specific De Geer ridges. Thus it is not
35 300 possible to establish whether an individual drumlin formed while the margin was only a few
36 301 hundred metres away in distal direction or some kilometres, as its orientation remains roughly
37 302 perpendicular to that of most De Geer ridges. Yet, since the orientation of the latter shifts
38 303 abruptly on either side of the Kumla-esker it is almost certain that the maximum distance
39 304 between the forming drumlins and the ice margin is represented by the distance to the esker.
40 305 This has to be measured along the once existing ice flowlines as evidenced by the small-scale
41 306 drumlins, and can be practically obtained by simply projecting down-flow the drumlin long
42 307 axis until this intercepts the esker. In the other direction a hypothetical flow line would
43 308 gradually fall into the primary N-S directed flow lines that are not influenced by the calving

1
2
3
4
5
6
7 309 bay configuration. The measured distances of this varies from 1 km in the south of the study
8 310 area (near the 'x' of the transect marked in Fig. 4), to 7.7 km, further north.

9
10 311 The concept of retreating margins ~~controlling setting~~ drumlin orientations has previously been
11 312 ~~discussed set out~~ by Mooers (1989). In a time-transgressive model of drumlin formation
12 313 located under the Rainy and Superior lobes of the Laurentide ice sheet, it was shown that the
13 314 trend of drumlin axes was primarily set by a retreating ice margin. However, Mooers' model
14 315 only located this within a distance of 20-30 km of said ice margin, rather than the more
15 316 proximal distance of approximately 1-7.7 km that we report here.

16
17
18
19 317 *Formation time*

20
21 318 Based on our proposed model of *where* the small-scale drumlins formed in relation to the ice
22 319 margin it is possible to calculate the time frame over which individual/adjacent near-marginal
23 320 drumlins were formed. This is a function of the time period over which the calving bay-
24 321 adjusted ice flow was operating over the ice-bed interface of the area in question. Therefore it
25 322 is possible to infer the maximum formation time from a known local ice recession rate.
26 323 Ideally we would be able to use the De Geer moraine ridges to do this, and this was the
27 324 original idea by De Geer (1989), i.e. that the ridges had geochronological significance in that
28 325 they were formed annually. This has also lately been suggested from a study of Swedish De
29 326 Geer moraines by Bouvier et al. (2015). However, such annuality has been rejected by, e.g.,
30 327 Hoppe (1959) and Strömberg (1965), as well as by Lindén and Möller (2005), who all argued
31 328 that multiple moraines could form within the same year. We thus ~~argue that we~~ cannot use the
32 329 mean distance between De Geer moraines in the Kumla-Örebro area as a reliable
33 330 chronometer.

34
35
36
37
38
39
40
41 331 However, it is possible to use the Swedish varve chronology to gain an appreciation of local
42 332 deglaciation time and the time frame over which the small-scale drumlins were formed. The
43 333 close to parallel and regularly spaced isochrones between -1200 and -900 over and north of
44 334 Stockholm (Fig. 1) suggest that these isochrones can, with a relatively high confidence, be
45 335 transferred laterally west-southwest-wards. This allows us to infer that the whole Kumla-
46 336 Örebro area was deglaciated between varve isochrones -1200 and -1100, i.e. in less than 100
47 337 years. This is then an absolute maximum time period for all the mapped small-scale drumlins
48 338 to form as their formation must have taken place during the passage of the Kumla-esker
49 339 calving bay, with their orientation showing an adjustment to this ice marginal configuration.
50 340 The 20 varve-year isochrones of Strömberg (1989) between years -1200/-1100 give an annual

1
2
3
4
5
6
7 341 mean steady state recession rate of ~220 m/yr. Although the recession rate value could have
8 342 varied locally along the gradually receding calving bay margin due to differences in calving
9 343 rates/events, ~~and therefore not be a steady-state retreat~~, we argue that it can be used as a good
10 344 average for the northwards propagation of the calving bay margin.

11
12
13 345 With this assumption in place the transect X-Y in Fig. 4 with a length of 7.7 km in the
14 346 Härminge and Brickebacken sub-areas, was deglaciated within ~30-35 years from the first
15 347 mapped De Geer moraine to the last. This was then a period that also time-transgressively
16 348 sustained the NE to SW-directed ice flow towards the eastern flank of the calving bay at
17 349 which point the smaller-scale drumlins were formed. A formation time of only a few decades
18 350 is further reinforced by the situation verified in the Stora Ulvgryta sub-area, on the opposite
19 351 side of the Kumla esker (Fig. 8). ~~A Here a SE-directed, and 5.3 km long, transect across the~~
20 352 ~~time transgressively formed~~ De Geer moraines draping the Stora Ulvgryta drumlins gives,
21 353 under the same assumptions as above, a deglaciation time of the whole transect of ~24 years.
22 354 The slight chronological difference between the two sides of the esker also demonstrates that
23 355 De Geer moraines are not a reliable chronometer for ice retreat rate. There are sections along
24 356 the X-Y transect (Fig. 4) over which there are very small spaces between the ridges (12
25 357 moraines over 1000 m; i.e. a mean spacing of 83 m) which means that the number of ridges
26 358 formed could have been as high as 2-3 ridges per year or even more over shorter steps of ice
27 359 margin retreat.

28
29
30
31
32
33
34
35 360 Our calculated period for the formation of the small-scale drumlins is a maximum time
36 361 period, referring as discussed above to the total deglacial age span with a sustained ice flow
37 362 direction from NE and NW ~~on either side of the Kumla esker, respectively~~. Should the
38 363 minimum distance to the ~~Kumla~~ esker of 1 km, verified for some of the drumlins, be taken
39 364 into consideration, the formation time of these features is reduced to only 5 years. This is
40 365 compatible with recent observations such as the repeat seismic and radar investigations under
41 366 the Antarctic Rutford Ice Stream, which revealed a 10 m high and 100 m wide streamlined
42 367 bedform forming/evolving within a period of only 7 years (Smith et al., 2007; King et al.,
43 368 2009). In agreement with these results there is also a recent study on the formation time of
44 369 drumlins at Fláajökull on Iceland (Jónsson et al., in press), similar in size to the ones analysed
45 370 here, with a suggested ~29 year formation time-frame. This is particularly interesting as a
46 371 modern example in a non-surge setting with a well-controlled formation time. The calculated
47 372 drumlin formation time of our study also fits within the broad time frame for drumlin
48 373 formation calculated by Rose (1989) of 8-292 years, falling within the lower end of that

1
2
3
4
5
6
7 374 range. The calculations by Rose (1989) build on sediment transfer rates applied to volume of
8 375 tills in their investigated drumlins; though an interesting approach this is hard to apply to the
9 376 drumlins described here. This is because the transfer rate of till for our region is largely
10 377 unknown and the volume of till in the drumlins is hard to evaluate as these features are likely
11 378 rock cored, as drumlins predominantly are in southern Sweden (Dowling et al., 2015).

12
13
14 379 In summary, the small-scale drumlins identified here formed ~1-7.7 km behind a retreating
15 380 calving bay ice margin and over formation periods of 5 to 35 years. The larger drumlins of the
16 381 area, which are an order of magnitude larger than the small-sized features and which are
17 382 parallel to the regional north to south-directed ice flow, should have formed over a much
18 383 longer period. Our reconstructions are further supported by the following lines of evidence:

19
20
21
22 384 (i) Smaller drumlins over-print the larger drumlins. The survival of the larger drumlins,
23 385 despite the near ice-marginal change in flow direction and subsequent sediment reorganisation
24 386 into the smaller drumlins shown here suggests that the duration of the flow event that created
25 387 the small-scale drumlins was not long enough, or lacked the erosive/deformative capacity, to
26 388 alter the orientation of the large drumlins.

27
28
29
30 389 (ii) The small-scale drumlins are only present in connection to closely spaced De Geer
31 390 moraines. This indicates that the small-scale drumlins only formed in places where the ice
32 391 margin had a quasi-stable ice retreat rate without large calving events that could have
33 392 generated large frontal retreats greater than several hundreds of metres.

34 35 36 37 393 **Conclusions**

38
39 394 We have found that small-scale drumlins in the Kumla–Örebro area are aligned – and thus
40 395 formed – parallel to flow lines that were adjusted to the configuration of calving embayments
41 396 in the receding ice margin at the last deglaciation. These embayments were located close to
42 397 the position of where larger eskers formed and were the product of enhanced calving at the
43 398 subaqueous outlets of the subglacial melt-water drainage. Furthermore, the area/calving
44 399 margin under which our mapped small-size drumlins formed was likely deglaciated over a
45 400 period of ~25-35 years, suggesting a maximum timeframe for their formation. To summarise,
46 401 the key findings of this paper are:

- 47
48
49
50
51
52 402 • Enhanced calving processes around the subaqueous outlets of well-developed
53 403 subglacial drainage networks caused marginal ice flow direction to converge towards

Formatted: Normal

1
2
3
4
5
6
7 404 the outlet/resulting esker. The result of this was the formation of calving bays and an
8 405 altered near-marginal ice flow direction. This is demonstrated by the geometric
9 406 relationship of drumlins, De Geer moraines and the Kumla esker in the studied area.

11
12 407 | • Mapped small-scale drumlins can form behind calving bays in response to the change
13 408 in flow direction. This has been verified in the Kumla-Örebro region where the
14 409 drumlins must have formed within c. 1-8 km of the active glacial margin.

17
18 410 | • Our studies suggest that drumlins of the size described can form under major ice-
19 411 sheets over very short time periods, 5-35 years.

22 412 **Acknowledgements**

23
24 413 The work presented here is part of a larger project (with P. Möller as PI) on formation of
25 414 streamlined terrain over south Sweden which, together with the papers by Dowling et al.
26 415 (2013), Dowling et al. (2015), Möller and Dowling (2015), Möller and Dowling (2016) and
27 416 Dowling et al. (2016) lead to, and are summarized in, the PhD thesis by Dowling (2016). The
28 417 LiDAR data used in this work is the property of Lantmäteriet (<http://www.lantmateriet.se>) and
29 418 is done so under agreement number: i2014 / 00579. Comments by JQS reviewers Julia
30 419 Wellner, [ClasClaes](#) Hättstrand and an anonymous reviewer greatly improved the focus of the
31 420 paper.

37 421 **References**

- 38
39 422 Bannerjee I, McDonald, BC. 1975. Nature of esker sedimentation. *In* Jopling, AV, McDonald,
40 423 BC. (eds.): Glaciofluvial and glaciomarine sedimentation. *SEPM Spec. Publ.* **23**:
41 424 132-154.
42 425 Benn DI, Evans DJA. 2010. *Glaciers and Glaciation*. Hodder Education, Euston Road,
43 426 London, UK: 802 p.
44 427 Benn DI, Hulton NRJ, Mottram RH. 2007^a. 'Calving laws, 'sliding laws' and the stability of
45 428 tidewater glaciers. *Annals of Glaciology* **46**: 123-130.
46 429 Benn DI, Warren CR, Mottram RH. 2007^b Calving processes and the dynamics of calving
47 430 glaciers. *Earth-Science Reviews* **82**: 143-179.
48 431 Bergdahl A. 1959. Glaciofluvial estuaries on the Närke plain. *Svensk Geografisk Årsbok* **35**:
49 432 47-70.

- 1
2
3
4
5
6
7 433 Bergdahl A. 1961. Det glaciala landskapet. Kumlabygden, Forn tid - Nutid – Framtid, del 1,
8 434 *Berg, jord och skogar*, 203-326. Kumla stad och Kumla Landskommun.
9
10 435 Bergdahl A. 1965. Isvikar och åsar i Kumla-Hallsbergsområdet. *Svensk Geografisk Årsbok*
11 436 **41**: 50-63.
12 437 Björck J, Possnert G, Schoning K. 2001. Early Holocene deglaciation chronology in
13 438 Västergötland and Närke, southern Sweden – biostratigraphy, clay varve, ¹⁴C and
14 439 calendar year chronology. *Quaternary Science Reviews* **20**: 1309-1326.
15 440 Björck S. 1995: A review of the history of the Baltic Sea, 13.0-8.0 ka BP. *Quaternary*
16 441 *International* **27**: 19-40.
17 442 Bouvier V, Johnsson M, Pässe T. 2015. Distribution, genesis and annual-origin of De Geer
18 443 moraines in Sweden: insights revealed by LiDAR. *GFF* **137**: 319-333.
19 444 Brunnberg L. 1995. Clay-varve chronology and deglaciation during the Younger Dryas and
20 445 Pre-boreal in easternmost part of the Middle Swedish Ice Marginal Zone. *Quaternaria*
21 446 *Series A:2 Thesis*: 95 pp.
22 447 Cato I. 1985. The definitive connection of the Swedish geochronological time scale with the
23 448 present, and the new date of the zero year in Döviken, northern Sweden. *Boreas* **14**:
24 449 117-122.
25 450 Cato I. 1987. On the definitive connection to the Swedish Time Scale with the present.
26 451 *Sveriges Geologiska Undersökning Ca* **68**: 55 pp.
27 452 Clark, CD. 2010. Emergent drumlins and their clones: from dilatancy to flow instabilities.
28 453 *Journal of Glaciology* **51**: 1011-1025.
29 454 Clark, CD., Hughes, AL., Greenwood, SL., Spagnolo, M. and Ng, FS., 2009. Size and shape
30 455 characteristics of drumlins, derived from a large sample, and associated scaling laws.
31 456 *Quaternary Science Reviews*, 28(7), pp.677-692.
32 457 Cook AG, Fox AJ, Vaughan DG, Ferrigno JG. 2005 Retreating glacier fronts on the Antarctic
33 458 Peninsula over the past half-century. *Science* **22**: 541-544.
34 459 De Geer G. 1989. Ändmoränerna i trakten mellan Spånga och Sundbyberg. *GFF* **11**: 395-396.
35 460 De Geer G. 1897. Om rullstensåsars bildningssätt. *Sveriges Geologiska Undersökning C* **197**:
36 461 25 pp. De Geer, G. 1940. Geochronologica Suecica Principles. *Kungliga Svenska*
37 462 *Vetenskapsakademiens handlingar 3dje Serien Bd* **18(6)**: 367 pp.
38 463 Dowling TPF. 2016. The drumlin problem – streamlined subglacial bedforms in southern
39 464 Sweden. *LUNDQUA Thesis* **80**: 1-32. Department of Quaternary Sciences/Department
40 465 of Geology, Lund University. (<https://lup.lub.lu.se/search/publication/8569667>)
41
42
43
44
45
46
47
48
49
50
51
52
53
54
55
56
57
58
59
60

- 1
2
3
4
5
6
7 466 Dowling TPF, Alexanderson H, Möller P. 2013. The new high-resolution LiDAR digital
8 467 height model ('Ny Nationell Höjdmodell') and its application to Swedish Quaternary
9 468 geomorphology. *GFF* **135**: 145-151.
- 10 469 Dowling TPF, Spagnolo M, Möller P. 2015. Morphometry and core type of streamlined
11 470 bedforms in southern Sweden from high resolution LiDAR. *Geomorphology* **236**: 54-
12 471 63.
- 13 472 Dowling TPF, Möller P, Greenwood S, Spagnolo M, Åkesson M, Hughes A, Frasier S, Clark
14 473 C. 2016. The extent to which geological factors influence the shape of streamlined
15 474 subglacial landforms. Submitted to *Geomorphology*. In Dowling TPF, The drumlin
16 475 problem – streamlined subglacial bedforms in southern Sweden. *LUNDQUA Thesis* **80**:
17 476 57-78. Department of Quaternary Sciences/Department of Geology, Lund University.
18 477 (<https://lup.lub.lu.se/search/publication/8569667>)
- 19 478 Ericsson B. 1979. Description to the Quaternary map Karlskoga SO. *Sveriges Geologiska*
20 479 *Undersökning Ae* **37**: 108 pp.
- 21 480 Fredén C. (ed.), 2009. *Berg och jord, Sveriges Nationalatlas* (4th ed.). Nordstedts Kartor AB,
22 481 Bromma, Sweden. 208 pp. ISBN 978-91-87760-56-3.
- 23 482 Fromm E. 1972. Description of the Geological map Örebro SV. *Sveriges Geologiska*
24 483 *Undersökning Ae* **5**: 100 pp.
- 25 484 Fromm E. 1991. Varve chronology and deglaciation in south-eastern Dalarna, central Sweden.
26 485 *Sveriges Geologiska Undersökning Ca* **77**: 49 pp.
- 27 486 Frödin G. 1916. Über einige spätglaziale Kalbungsbukten und fluvioglaziale Estuarien im
28 487 mittleren Schweden. *Bulletin Geologiska Institutionen, Upsala* **15**: 149-174.
- 29 488 Glückert G. 1973. Two large drumlin fields in central Finland. *Fennia* **120**: 37 pp.
- 30 489 Glückert G. 1987. The drumlins of central Finland. Pp. 291-307 in Menzies, J. & Rose, J.
31 490 (eds.): *Drumlin Symposium*. A. A. Balkema. 360 pp.
- 32 491 Hoppe G. 1948. Isrecessionen från Norrbottens Kustland i belysningen av de glaciala
33 492 formelementen. *Geographica* **20**: 112 pp. (Uppsala University, Department of
34 493 Geography)
- 35 494 Hoppe G. 1957. Problems of glacial geomorphology and the ice age. *Geografiska Annaler* **39**:
36 495 1-18.
- 37 496 Hoppe G. 1959. Glacial morphology and inland ice recession in northern Sweden.
38 497 *Geografiska Annaler* **41**: 193–212.

- 1
2
3
4
5
6
7 498 Hättestrand C, Götz S, Näslund JO, Fabel D, Stroeven AP. 2004. Drumlin formation time:
8 499 evidence from northern and central Sweden. *Geografiska Annaler: Series A, Physical*
9 500 *Geography* 86, 155-167.
- 10 501 Johnson MD, Schomacker A, Benediktsson ÍÖ, Geiger AJ, Ferguson A, Ingólfsson Ó. 2010.
11 502 Active drumlin field revealed at the margin of Múlajökull, Iceland: a surge-type
12 503 glacier. *Geology* 38(10): 943-6.
- 13 504 Jónsson SA, Benediktsson ÍÖ, Ingólfsson Ó, Schomacker A, Bergsdóttir HL, Jacobson jr WR,
14 505 Linderson H. (*in press*). Submarginal drumlin formation and late Holocene history of
15 506 Fláajökull, southeast Iceland. *Annals of Glaciology*
- 16 507 King, EC, Hindmarsh, RC, Stokes, C. 2009. Formation of mega-scale glacial lineations
17 508 observed beneath a West Antarctic ice stream. *Nature Geoscience* 2, 585-588.
- 18 509 Kranck, K. 1973. Flocculation of suspended sediment in the sea. *Nature* 246, 348-350.
- 19 510 Lamsters K, Zelčs V. 2015. Subglacial landforms of the Zemgale Ice Lobe, south-eastern
20 511 Baltic. *Quaternary International* 386: 42-54
- 21 512 Lindén M, Möller P. 2005. Marginal formation of De Geer moraines and their implications to
22 513 the dynamics of grounding-line recession. *Journal of Quaternary Science* 20: 113-133.
- 23 514 Lundqvist J. 2009. Weichsel-istidens huvudfas. In *Berg och jord, Sveriges Nationalatlas*,
24 515 Fredén C. (ed.). Nordstedts Kartor AB, Bromma, Sweden. (4th ed.): 124-135. ISBN
25 516 978-91-87760-56-3.
- 26 517 Magnusson E. 1984. Description to the Quaternary map Västerås SO. *Sveriges Geologiska*
27 518 *Undersökning Ae* 64: 76 pp.
- 28 519 Mangerud J, Gyllenkreutz R, Lohne Ø, Svendsen JI. 2011. Glacial history of Norway. In
29 520 *Quaternary Glaciations - Extent and Chronology - a closer look*, Ehlers J., Gibbard
30 521 PL, Hughes, PH (eds.), *Developments in Quaternary Science* 15: 279-298. Elsevier.
- 31 522 Menzies J. 1979. A review on the literature on the formation and location of drumlins. *Earth*
32 523 *Science Reviews* 14: 315-359.
- 33 524 Mooers HD. 1989. Drumlin formation: a time transgressive model. *Boreas* 18, 99-107.
- 34 525 Möller P, Dowling TPF. 2016: Streamlined subglacial bedforms on the Närke plain, south-
35 526 central Sweden – areal distribution, morphometrics, internal architecture and
36 527 formation. *Quaternary Science Reviews* X: xx-xx (accepted).
- 37 528 Napieralski J, Nalepa N. 2010. The application of control charts to determine the effect of
38 529 grid cell size on landform morphometry. *Computers & Geosciences* 36: 222-230.
- 39 530 Nilsson E. 1968. Södra Sveriges senkvartära historia. *Geokronologi, issjöar och landhöjning*.
40 531 *Kungliga Svenska Vetenskapsakademins Handlingar*, 4th ser., vol. 12: 117 pp.

- 1
2
3
4
5
6
7 532 Raukas A, Tavast E. 1994. Drumlin location as a response to bedrock topography on the
8 533 southeastern slope of the Fennoscandian Shield. *Sedimentary Geology* **91**: 373-382.
9
10 534 Rose, J. 1989. Glacier stress patterns and sediment transfer associated with the formation of
11 535 superimposed flutes. *Sedimentary Geology* **62**: 151-176.
12 536 Skei JM, Syvitski JPM. 2013. Natural flocculation of mineral particles in seawater – influence
13 537 on mine tailing sea disposal and particle dispersal. *Mineralproduktion* **3**:A1-A10.
14 538 Smith AM, Murray T, Nicholls KW, Makinson K, Aðalgeirsdóttir G, Behar AE, Vaughan
15 539 DG. 2007. Rapid erosion, drumlin formation, and changing hydrology beneath an
16 540 Antarctic ice stream. *Geology* **35**: 127-130.
17
18 541 Spagnolo M, Clark CD, Hughes ALC. 2012. Drumlin relief. *Geomorphology* **153-154**: 179-
19 542 191.
20
21 543 Stokes CR, Fowler AC, Clark CD, Hindmarsh RC, Spagnolo M. 2013. The instability theory
22 544 of drumlin formation and its explanation of their varied composition and internal
23 545 structure. *Quaternary Science Reviews* **62**, 77-96.
24
25 546 Stokes CR, Spagnolo M, Clark CD. 2011. The composition and internal structure of drumlins:
26 547 complexity, commonality, and implications for a unifying theory of their formation.
27 548 *Earth-Science Reviews* **107**: 398-422.
28
29 549 Stroeven AP, Heyman J, Fabel D, Björck S, Caffee MW, Fredin O, Harbor JM. 2015. A new
30 550 Scandinavian reference ¹⁰Be production rate. *Quaternary Geochronology* **29**:104-115.
31
32 551 Stroeven AP, Hätttestrand C, Kleman J, Heyman J, Fabel D, Fredin O, Goodfellow BW,
33 552 Harbor JM, Jansen JD, Olsen L, Caffee MW, Fink D, Lundqvist J, Rosqvist GC,
34 553 Strömberg B, Jansson KN. 2015. Deglaciation of Fennoscandia. *Quaternary Science*
35 554 *Reviews X*: xx-xx (in press).
36
37 555 Strömberg B. 1965. Mapping and geochronological investigations in some moraine areas of
38 556 south-central Sweden. *Geografiska Annaler* **47A**: 73-82.
39
40 557 Strömberg B. 1981. Calving bays, striae and moraines at Gysinge-Hedesunda, central
41 558 Sweden. *Geografiska Annaler* **63A**: 149-154.
42
43 559 Strömberg B. 1989. Late Weichselian deglaciation and clay varve chronology in east-central
44 560 Sweden. *Sveriges Geologiska Undersökning Ca* **73**: 70 pp.
45
46 561 Strömberg B. 1994. Younger Dryas deglaciation at Mt Billingen, and clay varve dating of the
47 562 Younger Dryas/Preborial transition. *Boreas* **23**:177-193.
48
49 563 Svendsen JI, Alexanderson H, Astakhov VI, Demidov I, Dowdeswell JA, Funder S, Gataulin V,
50 564 Henriksen M, Hjort C, Houmark-Nielsen M, Hubberten HW, Ingólfsson Ó, Jakobsson
51 565 M. Kjær KH, Larsen E, Lunkka JP, Lyså A, Mangerud J, Matushkov A, Murray A,

- 1
2
3
4
5
6 566 Möller P, Niessen F, Nikolskaya O, Polyak L, Saarnisto M, Siegert C, Siegert MJ,
7 Spielhagen RF, Stein R. 2004. The Late Weichselian Quaternary ice sheet history of
8 567 northern Eurasia. *Quaternary Science Review* **23**: 1229–1271.
9 568
10 569 Warren WP, Ashley GM. 1994. Origins of the ice-contact stratified ridges (eskers) of Ireland.
11 570 *Journal of Sedimentary Research* **A64**: 433-449.
12 571 Wellner JS, Lowe AL, Shipp SS, Anderson JB. 2001. Distribution of glacial geomorphic
13 572 features on the Antarctic continental shelf and correlation with substrate: implications
14 573 for ice behavior. *Journal of Glaciology* **47**: 397-411.
15 574 Venteris, E.R. 1999 Rapid tidewater glacier retreat: a comparison between Columbia Glacier,
16 575 Alaska and Patagonian calving glaciers. *Global and Planetary Change* **22**: 131-138.
17 576
18
19
20
21
22
23
24
25
26
27
28
29
30
31
32
33
34
35
36
37
38
39
40
41
42
43
44
45
46
47
48
49
50
51
52
53
54
55
56
57
58
59
60

577 Captions and Tables

578

	<i>n</i>	Mean Height	Height P ₁₀	Height P ₉₀	Mean Length	Length P ₁₀	Length P ₉₀	Mean Width	Width P ₁₀	Width P ₉₀	Mean Orientation
<i>Area 1</i>	48	0.9	0.4	1.8	113.5	64.8	188.8	31	15.3	57.6	35-215
<i>Area 2</i>	155	1.5	0.8	2.3	112.7	68.4	175.3	33	17.7	56.4	30-210
<i>Area 3</i>	54	1.8	1	3	117.4	65	240.8	40.4	22.2	70.8	210-30

579

580 Table 1. Summary statistics for flow set morphometrics. All values are in meters and rounded
581 to 1 decimal point. Mean orientation is given to the nearest whole degree, the values
582 representing the orientation of the a-axis, with the upstream polarity given first.

583 Fig. 1. (A) Overview of NW Europe. Red dashed line = proposed Fennoscandian Ice Sheet
584 margin to the west/south at LGM (Svendsen et al., 2004); blue dashed line = the Younger
585 Dryas Ice Marginal Zone (Mangerud et al., 2011). (B) Map of southern Sweden (for location,
586 white box in (A)), showing areas above and below the highest shoreline (marine limit in the
587 west), and altitude of the highest shoreline at deglaciation. The highest shoreline east of
588 Billingen is the shore altitude for the Baltic Ice Lake prior to its 2nd drainage at retreat from
589 Billingen after the Younger Dryas advance, while highest shoreline isobases north thereof
590 were formed in the following Baltic Basin stages Yoldia Sea and Ancylus Lake (Björck,
591 1995), following the northwards receding ice margin. Inferred ice-marginal positions during
592 the Younger Dryas are according to Lundqvist (2009). Deglacial varve isochrones are
593 transferred from Brunberg (1995) (south of Stockholm), Strömberg (1994) (Lake Vänern-
594 Askersund) and Strömberg (1989) (north of Stockholm). Base map compiled from the
595 Swedish National Atlas (Fredén, 2009). Red box marks the investigated area between Örebro
596 and Kumla (Fig. 3) and orange boxes mark the positions of Figs. 2A and 2B. Typical ice flow
597 for the local area was north-south.

598 Fig. 2. Examples of reconstructed calving bays around some of the larger eskers north of
599 Lake Mälaren, south-central Sweden (Fig. 1B), based on varved clay measurements (redrawn
600 from Plates 2 and 3 in Strömberg (1989)). Eskers are shown in green, striae outcrop locations
601 are marked with a red with the direction indicated by the red line and the black lines indicate
602 varve-Varve isochrones. The latter are based on lateral correlation of basal varves and are
603 drawn with 20 years interval. Indicated, and indicated varve years for deglaciation is in the
604 relation to the so called 'zero year' in the Swedish varved clay chronology (Cato 1985, 1987).
605 Measured youngest striae are marked from opposite sides of the esker/calving bays, indicating
606 near-marginal ice flow re-adjustment (from the general ice flow direction north to south),
607 being approximately perpendicular to the calving bay configuration at ice-margin gradual
608 retreat. (A) The moderately indented calving bay gradually forming around the Uppsala esker
609 at ice recession between varve years -1100 and -920 (180 years) over a distance of ~40 km
610 (mean recession ~222 m/year). Note a slight increase with time in calving bay depth towards
611 the north. Calving bay depths and widths are hard to define, but depths are only in the order of

20

1
2
3
4
5
6
7 612 2-4 km, marked as shallow indentions in the close to west to east-trending receding ice margin.
8 613 Centre of the map is N59°43'; E17°36' (position marked with orange box in Fig. 1B). (B)
9 614 The strongly but variably indented calving bays gradually forming around the Enköping and
10 615 Gävle eskers at ice recession between varve years -800 and -700 (100 years) over a distance
11 616 of ~47 km (mean recession ~470 m/year). Calving bay depths north of isochrone -800 vary
12 617 between 6-15 km and widths between 6-17 km at bay mouths, with both calving bay depth
13 618 decreases and increases at gradual ice margin recession. Centre of the map is N60°25';
14 619 E16°53' (position marked with orange box in Fig. 1B).

16 620 Fig. 3. Overview of Quaternary sediments and landforms in the Kumla-Örebro area. (A)
17 621 Extract of the Quaternary geology map Örebro SW (Fromm, 1972). For full legend, see online
18 622 version at <http://resource.sgu.se/produkter/ae/ae5-karta.pdf>. (B) Extract of De Geer moraines
19 623 (blue lines), eskers (green) and youngest striae (red bullet arrows) from (A). The north to
20 624 south trending Kumla esker has nearby De Geer moraines trending towards WSW to SW west
21 625 of the esker, while De Geer moraines east of the esker trend towards SE, indicating local ice
22 626 margin rearrangement from the general W-E trend around the esker and thus suggesting the
23 627 formation of a calving bay at the northwards retreat of the subaqueous ice margin (Bergdahl
24 628 1959, 1965; Fromm 1972). Place names Härminge, Brickebacken and Stora Ulvgryta, and
25 629 their black frames, indicate the positions of LiDAR-derived DEM scenes shown in Figs. 5, 7
26 630 and 8, revealing much denser patterns of De Geer moraines than shown here as based on
27 631 ground survey mapping.

30 632 Fig. 4. Overview LiDAR-based mapping of drumlins and De Geer moraines in the Kumla-
31 633 Örebro area (the same geographic extent as in Fig. 3). Drumlins are divided into large-scale
32 634 drumlins (black outlines) showing the same N-S trend as for the rest of the streamlined flow
33 635 sets of the Närke plain (Möller and Dowling, accepted), while the small-scale drumlins (red)
34 636 when occurring deviate from this regional direction, trending NW-SE and NE-SW on the
35 637 respective sides of the Kumla esker. De Geer moraines are perpendicular to the small-scale
36 638 drumlins and thus trend NE-SW and NW-SE on opposite sides of the said esker. Coverage of
37 639 the three zoomed in Lidar DEM's in Figs. 5, 7 and 8 are marked by black frames.

40 640 Fig. 5. LiDAR-based mapping of small-scale drumlins and De Geer moraines in the Härminge
41 641 subarea (geographic coverage shown in Fig. 4). Hillshade illumination is from 120° with an
42 642 azimuth of 25° and an x5 vertical exaggeration. ~~The colour ramp has been inverted.~~

44 643 Fig. 6. A drone image (view towards NE) of De Geer moraines in the Härminge subarea
45 644 (Figs. 4 and 5). Five De Geer moraine ridges are here protruding through surrounding clay,
46 645 which are the agricultural fields in the fore- and mid-ground. The moraine closest to the
47 646 viewer is approximately 50 m long. The ridges trend NW-SE and tentative ice margins at their
48 647 formation are indicated by white hatched lines.

50 648 Fig. 7. LiDAR-based mapping of small-scale drumlins and De Geer moraines in the
51 649 Brickebacken subarea (geographic coverage shown in Fig. 4). Hillshade illumination is from
52 650 120° with an azimuth of 25° and an x5 vertical exaggeration. The colour ramp has been
53 651 inverted.

1
2
3
4
5
6
7 652 Fig. 8. LiDAR-based mapping of small-scale drumlins and De Geer moraines in the Stora
8 653 Ulvhytta subarea (geographic coverage shown in Fig. 4). Hillshade illumination is from 250°
9 654 with an azimuth of 25° and an x5 vertical exaggeration. The colour ramp has been inverted.

10 655 Fig. 9. Idealised ice flow re-organisation and calving bay formation (left-hand scenes). The
11 656 selected area is a random snapshot of the main Kumla esker body (pannels A, C and E), along
12 657 with an idealised geomorphological evolution sketch map (pannels B, D and F). The area in
13 658 front of the depicted calving embayments was occupied by the marine Yoldia Sea with water
14 659 depths in the order of 80-130 m. (A) Flow lines further back from the ice margin at formation
15 660 of the large-scale streamlined bed forms. (B) Large drumlinoids (black ellipses) developed
16 661 parallel to the regional ice flow direction further back from the receding ice margin. (C-D) A
17 662 calving bay is formed at ice margin recession (arbitrarily chosen time-transgressive position),
18 663 in which apex the esker (green line) formed as lined-up subaqueous fans at the subglacial
19 664 tunnel mouth. Ice flow (indicated by blue flow lines) was re-arranged from regional flow to
20 665 be adjusted perpendicular to the new ice margin configuration of the approaching calving bay.
21 666 De Geer moraines (blue lines) formed gradually at the receding ice margin at an ~30-35°
22 667 angle to the N-S directed esker. Small-scale drumlins (red) formed parallel to the near-
23 668 marginal flow lines. (E-F) The final stages of the calving bay, the bay has opened out and ice
24 669 flow is readjusting to a north-south direction. No small drumlins are seen to form with this
25 670 flow orientation. The De Geer moraines formed at this stage are not perpendicular to the small
26 671 drumlins formed early on.

27
28
29
30 672
31
32
33
34
35
36
37
38
39
40
41
42
43
44
45
46
47
48
49
50
51
52
53
54
55
56
57
58
59
60